X Зимняя школа по теоретической физике

Дубна, 4 февраля 2012

Столкновения тяжелых ионов на LHC

А.В. Леонидов

Физический институт РАН

QCD phase diagram

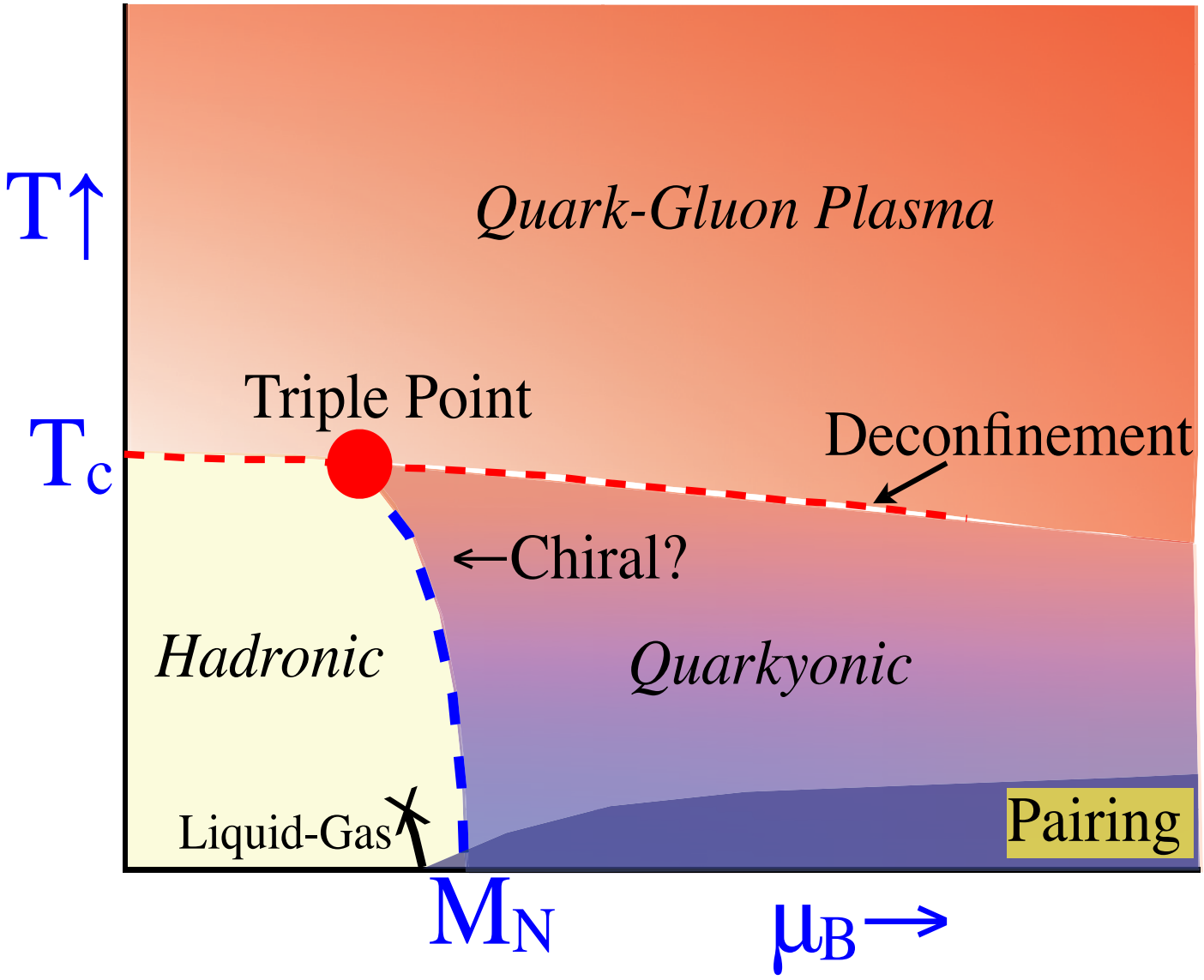

QCD phase diagram

- Transverse mass:

$$m_T = \sqrt{p_T^2 + m^2}$$

- Thermal transverse spectrum:

$$\frac{1}{2\pi}\frac{dN_i}{p_T dp_T dy} = \frac{1}{2\pi}\frac{dN_i}{m_T dm_T dy} = A_i \mathrm{e}^{-m_T^i/T}$$

- Blue-shifted temperature:

$$T = T_F \left(\frac{1+\langle v_T\rangle}{1-\langle v_T\rangle}\right)^{1/2}$$

- $\langle v_T\rangle$: average velocity of transverse expansion

QCD phase diagram

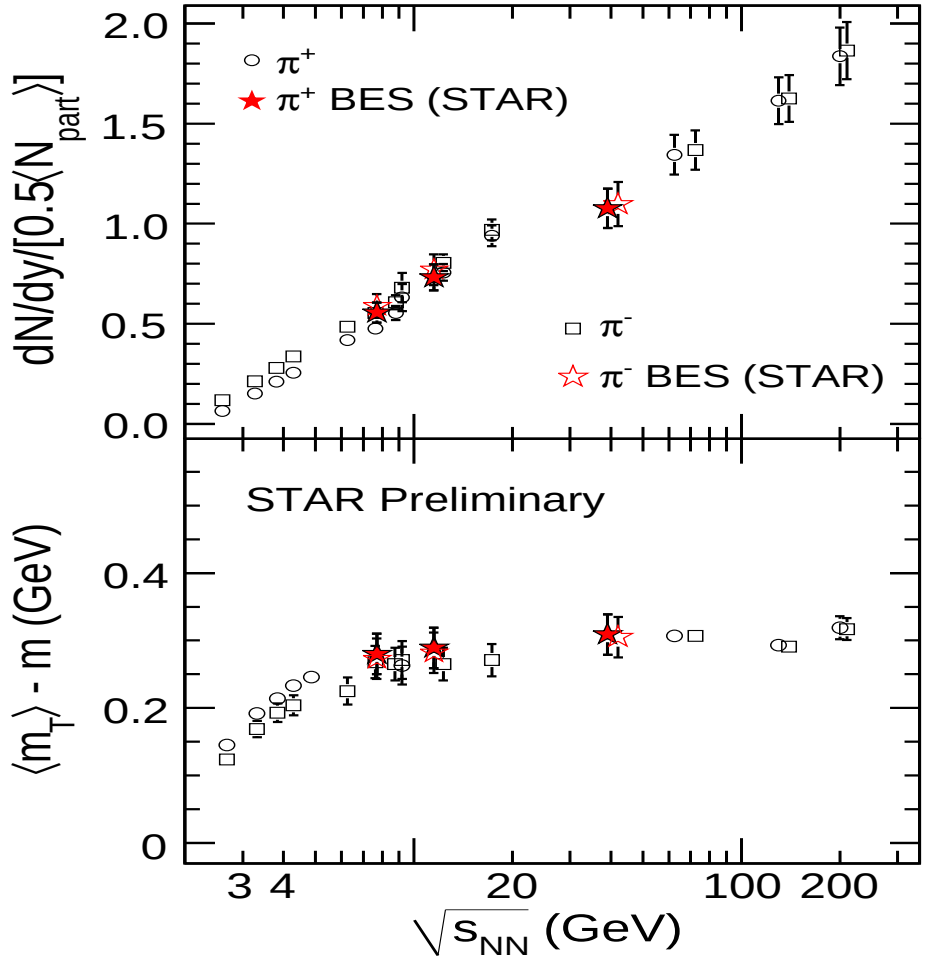

QCD phase diagram

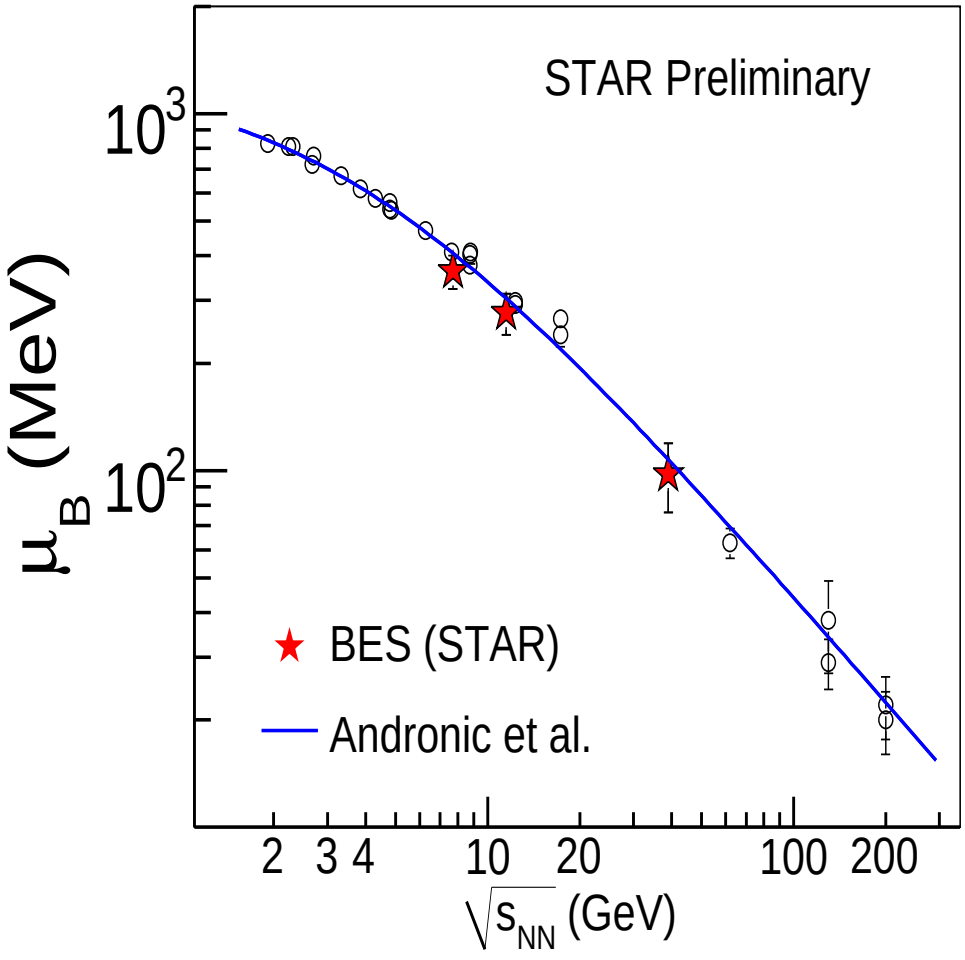

Baryon chemical potential as a function of $\sqrt{s}$

QCD phase diagram

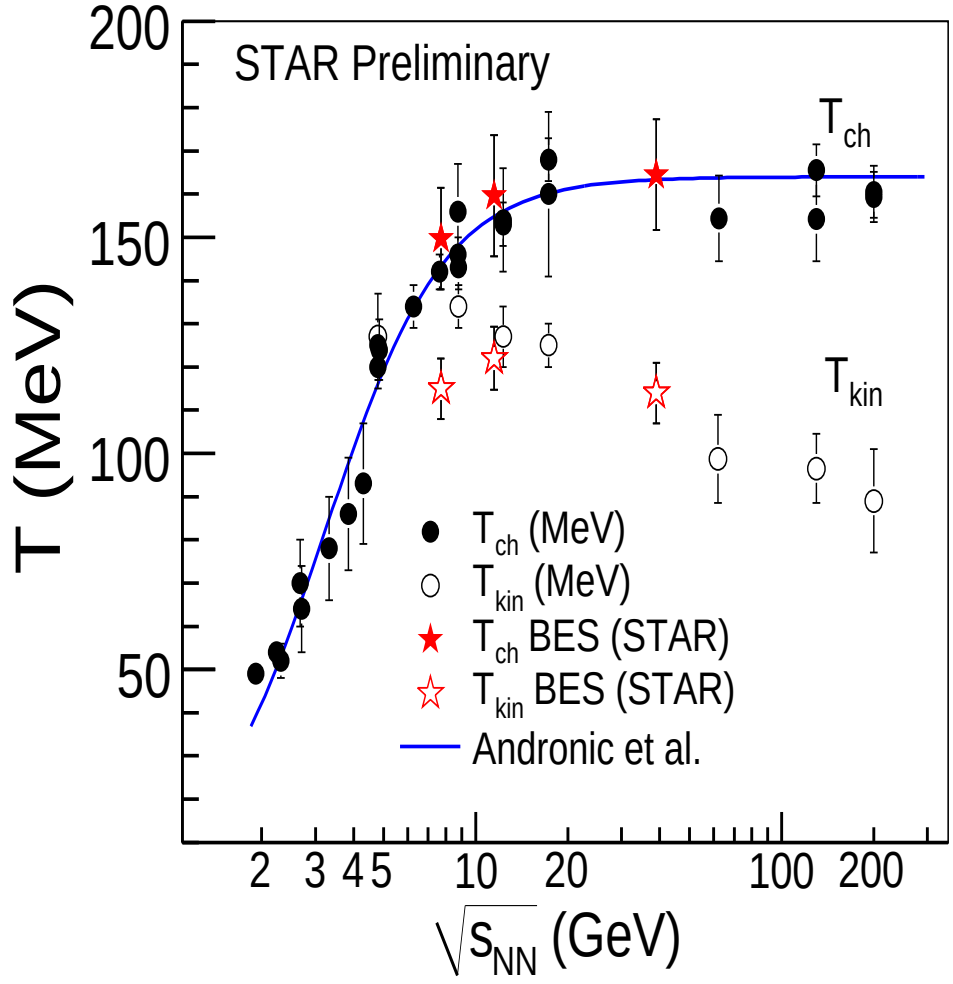

Kinetic and chemical freeze-out temperatures as functions of $\sqrt{s}$

QCD phase diagram

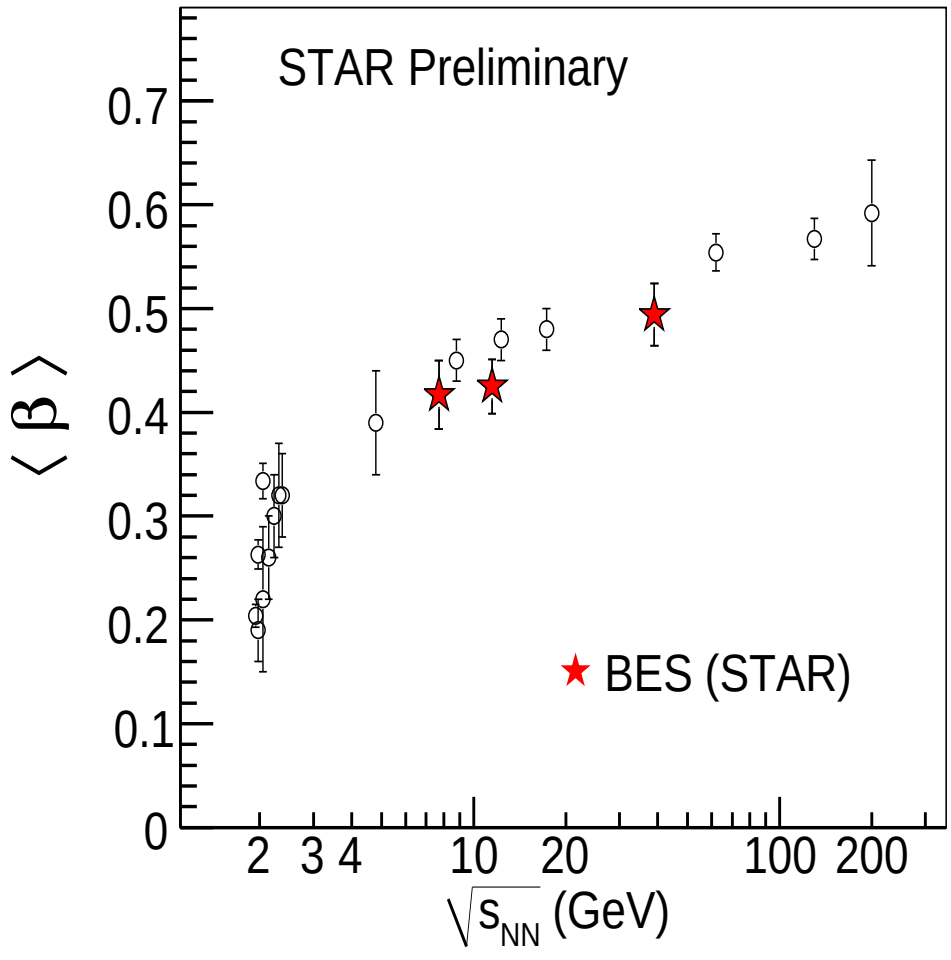

Average flow velocity as a function of $\sqrt{s}$

Stages of nuclear collisions

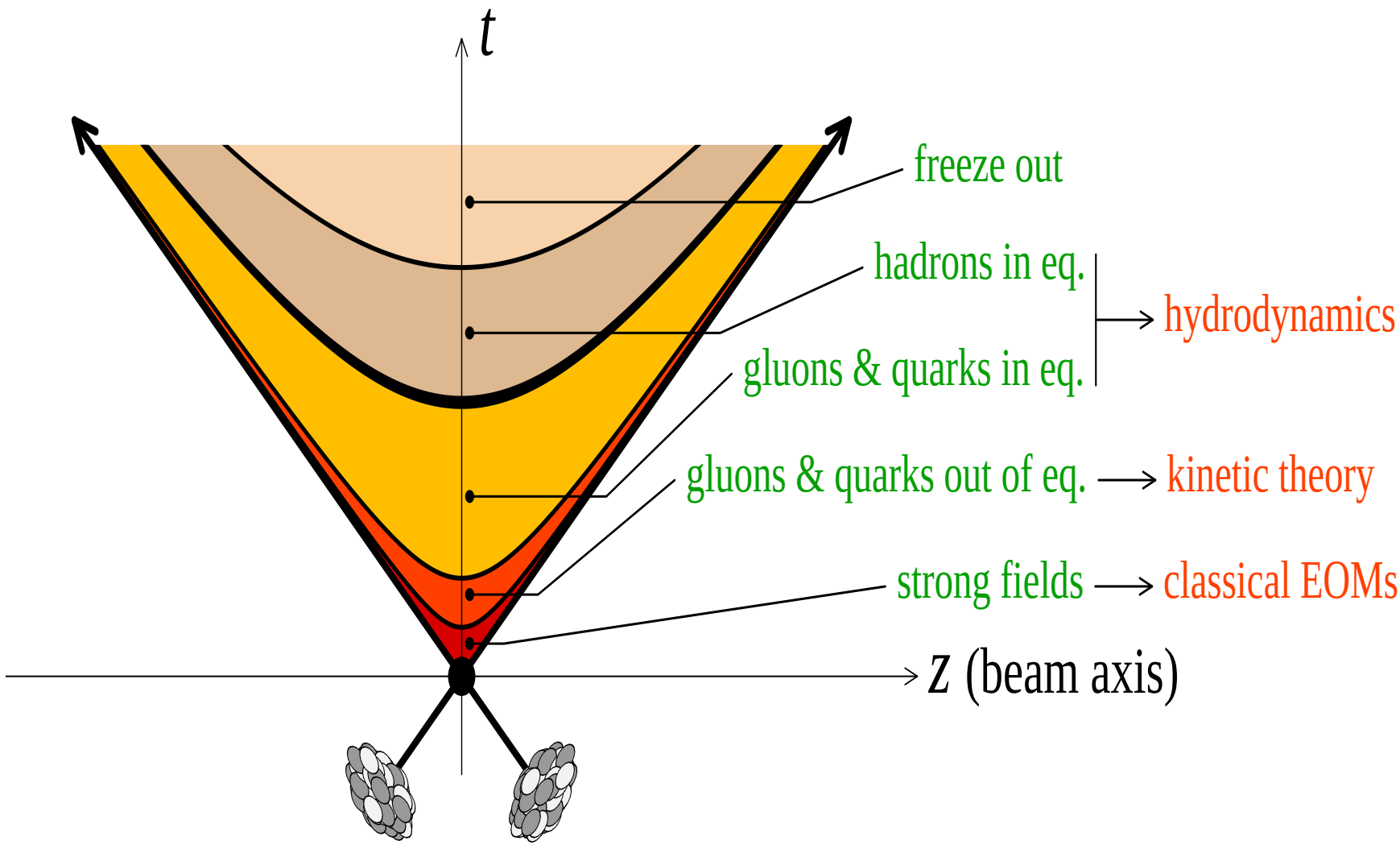

Glauber geometry

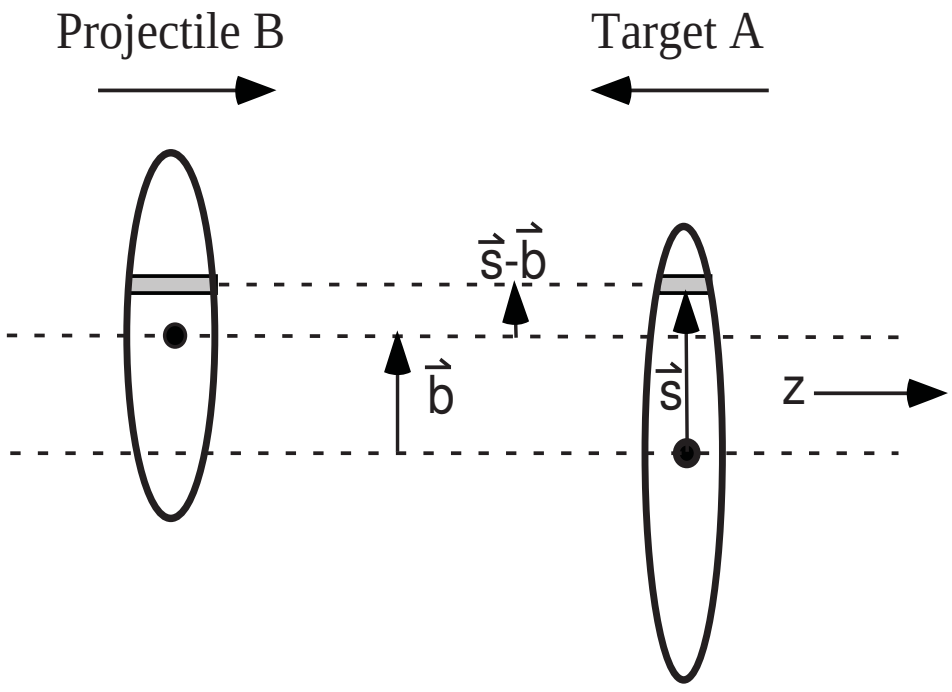

a) Side View

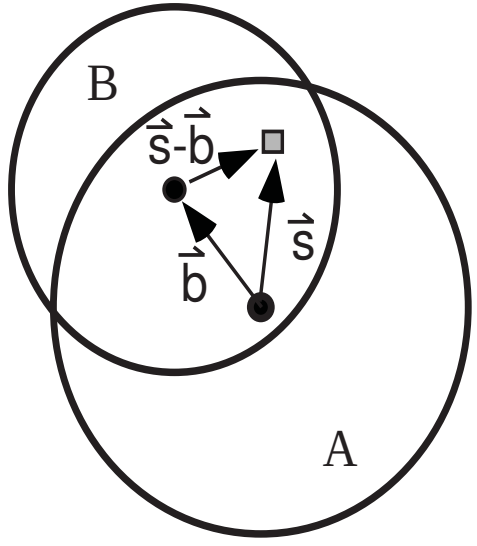

b) Beam-line View

Glauber geometry

- Исходная величина - плотность вероятности (на единицу площади) того, что *заданный* нуклон находится в рассматриваемой трубке:

$$t_A(\mathbf{s}) = \int dz_A \, \rho_A(\mathbf{s}, z_A)$$

- Плотность вероятности того, что *заданные* нуклоны в ядрах A и B находятся в нужных трубках

$$t_A(\mathbf{s}) \cdot t_B(\mathbf{s} - \mathbf{b}) d^2 s$$

- Функция перекрытия (thickness function)

$$t_{AB}(\mathbf{b}) = \int d^2 s \, t_A(\mathbf{s}) \cdot t_B(\mathbf{s} - \mathbf{b})$$

Glauber geometry

- Вероятность парного взаимодействия

$$p(1, \mathbf{b}) \;=\; t_{AB}(\mathbf{b})\, \sigma_{\text{in}}^{NN}$$

- Вероятность n взаимодействий

$$p(n, \mathbf{b}) = C_n^{AB} \left[t_{AB}(\mathbf{b})\, \sigma_{\text{in}}^{NN} \right]^n \left[1 - t_{AB}(\mathbf{b})\, \sigma_{\text{in}}^{NN} \right]^{AB-n}$$

Glauber geometry

- Полная вероятность взаимодействия

$$\frac{d^2\sigma_{\text{in}}^{A+B}}{d^2b} = \sum_{n=1}^{AB} p(n,\mathbf{b}) = 1 - [1 - t_{AB}(\mathbf{b})\,\sigma_{\text{in}}^{NN}]^{AB}$$

- Неупругое сечение ядро-ядро

$$\sigma_{\text{in}}^{A+B} = \int d^2b \left\{1 - [1 - t_{AB}(\mathbf{b})\,\sigma_{\text{in}}^{NN}]^{AB}\right\}$$

- Неупругое сечение протон-ядро

$$\sigma_{\text{in}}^{1+B} = \int d^2s \left\{1 - [1 - t_{A}(\mathbf{s})\,\sigma_{\text{in}}^{NN}]^{A}\right\}$$

Glauber geometry

- Число парных соударений

$$N_{\rm coll}(\mathbf{b}) = \sum_{n=1}^{AB} np(n,\mathbf{b}) = ABt_{AB}(\mathbf{b})\sigma_{\rm in}^{NN}$$

- Число взаимодействующих нуклонов

$$\begin{aligned} N_{\rm part} &= A\int d^2s\, t_A(\mathbf{s})\left\{1-\left[1-t_B(\mathbf{s}-\mathbf{b})\sigma_{\rm in}^{NN}\right]\right\} + \\ &\quad B\int d^2s\, t_A(\mathbf{s}-\mathbf{b})\left\{1-\left[1-t_A(\mathbf{s})\sigma_{\rm in}^{NN}\right]\right\} \end{aligned}$$

Glauber geometry

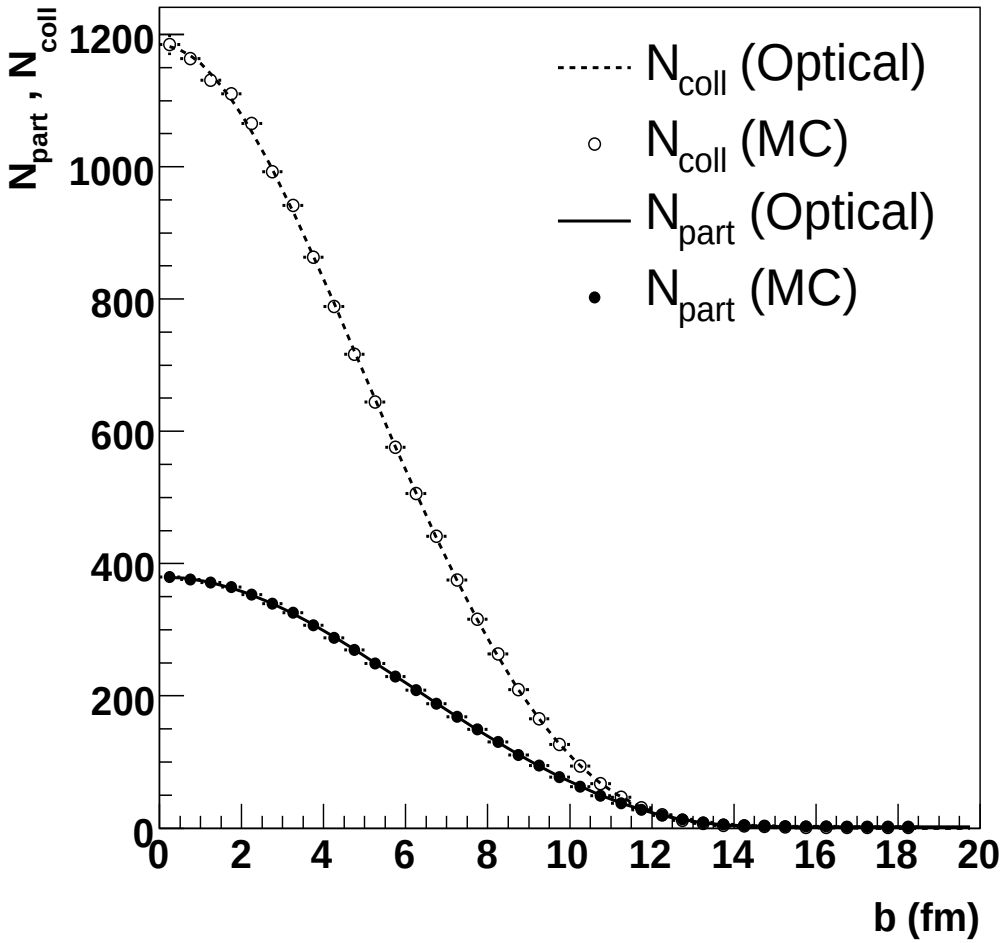

Binary vs wounded

Glauber geometry

Classification in centrality

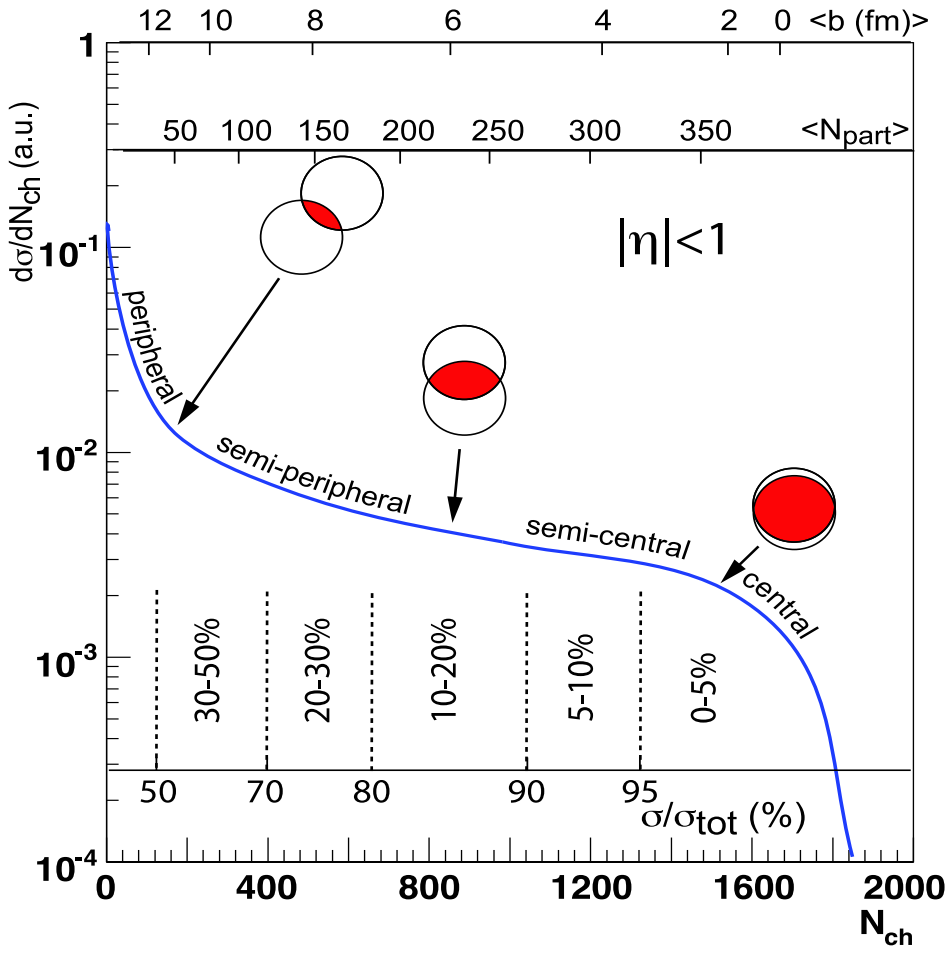

Particle multiplicity

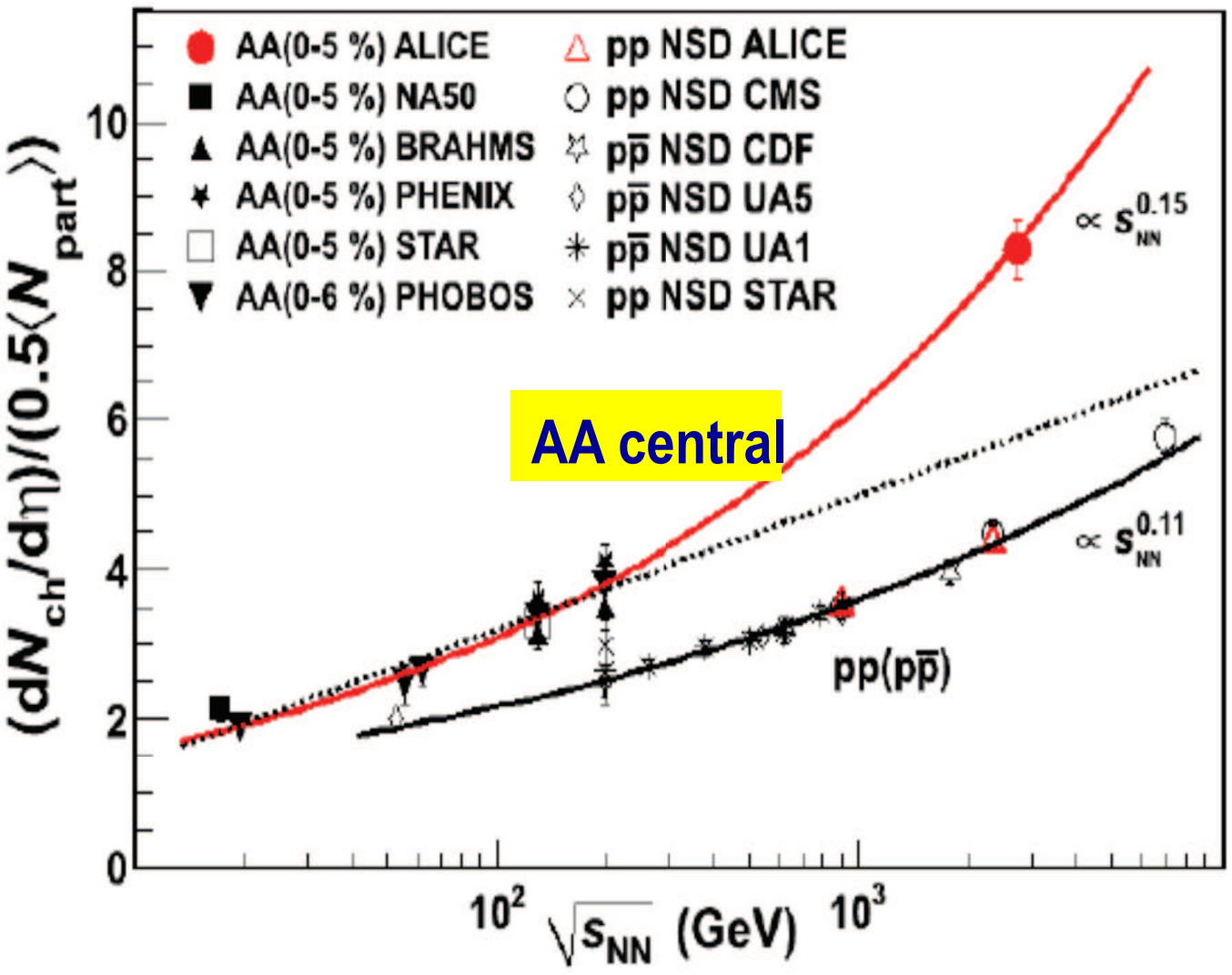

Multiplicity at $y = 0$ as a function of $\sqrt{s}$

Particle multiplicity

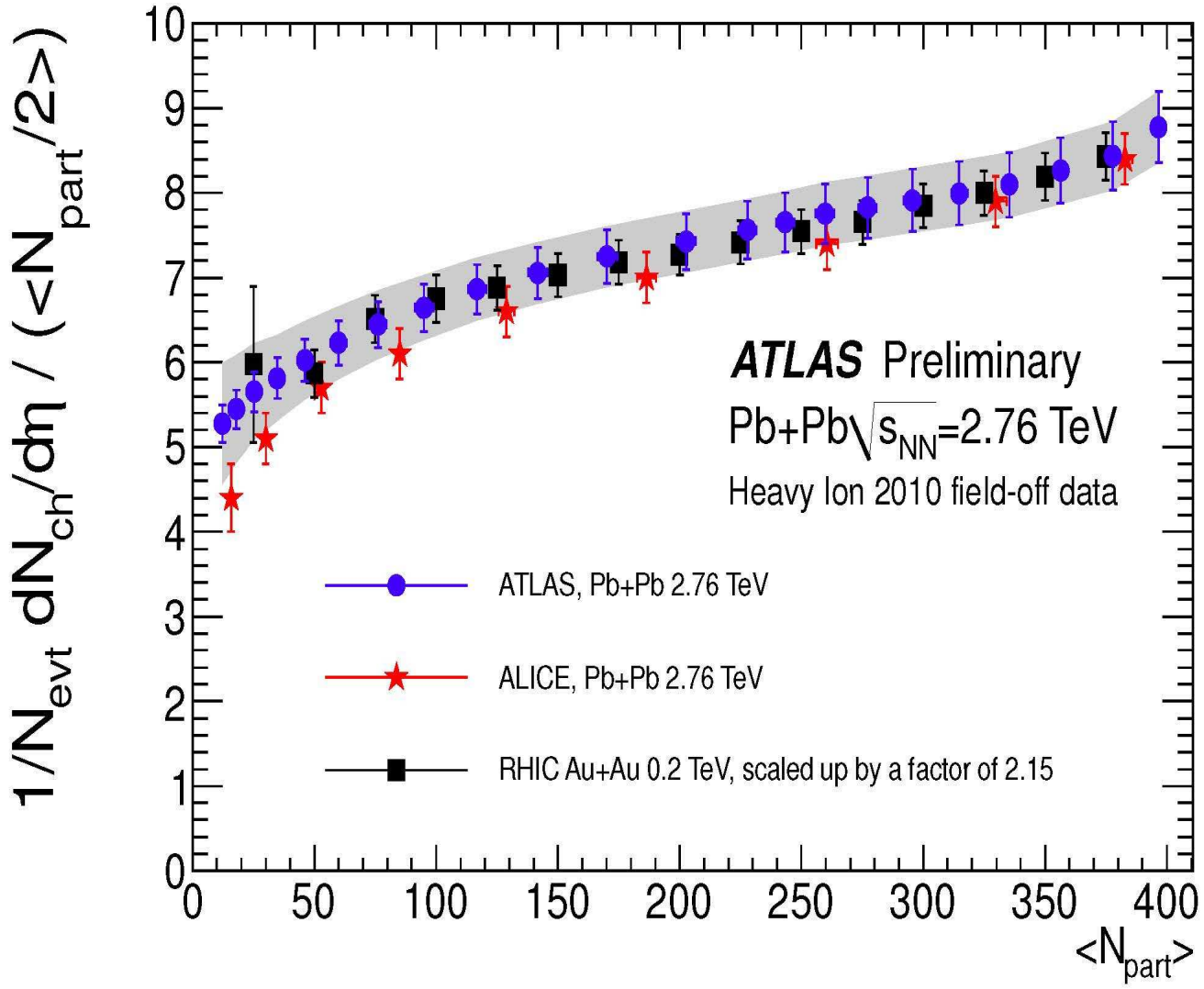

Multiplicity: centrality dependence

Particle spectra

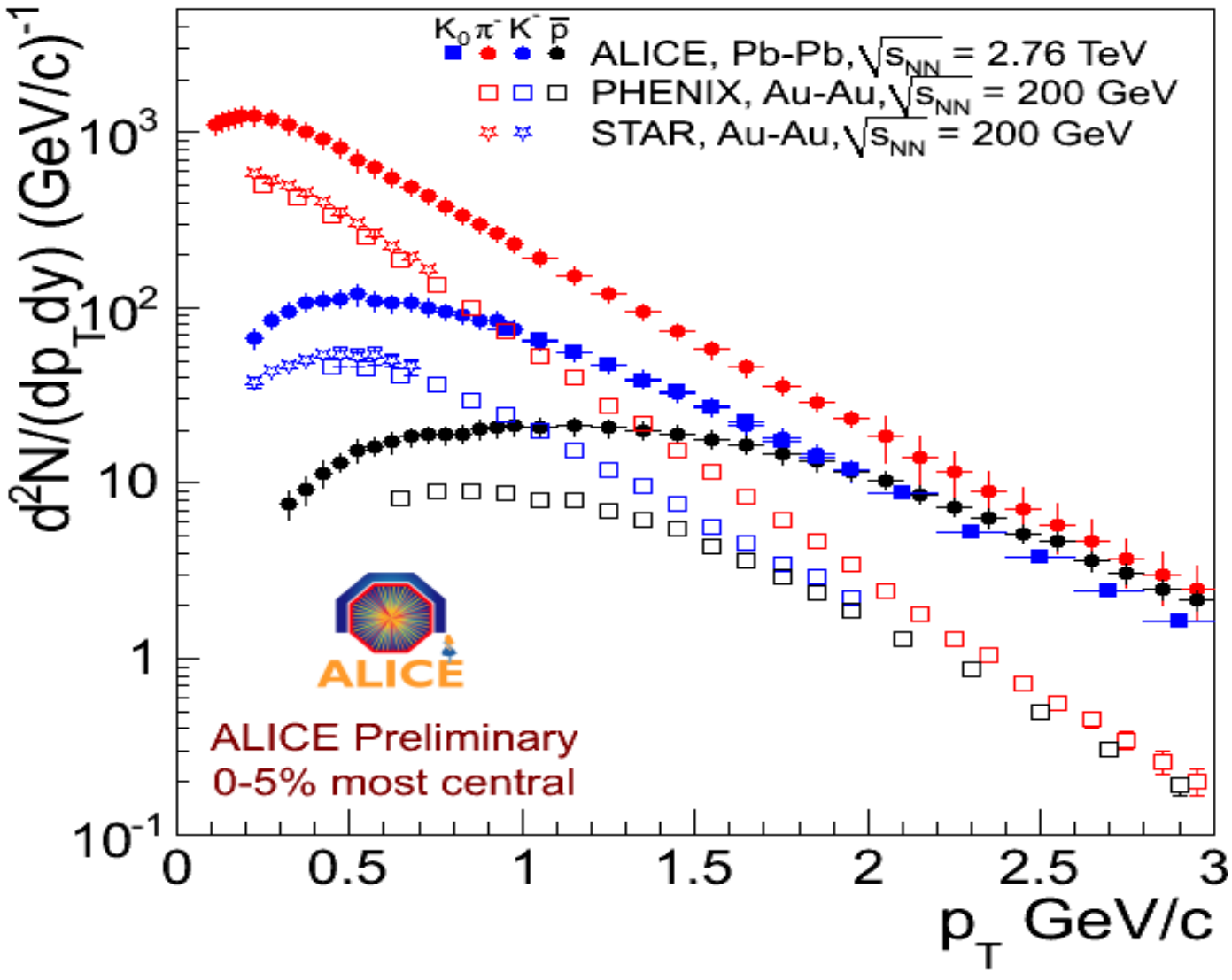

Particle spectra in p_T

Jet quenching

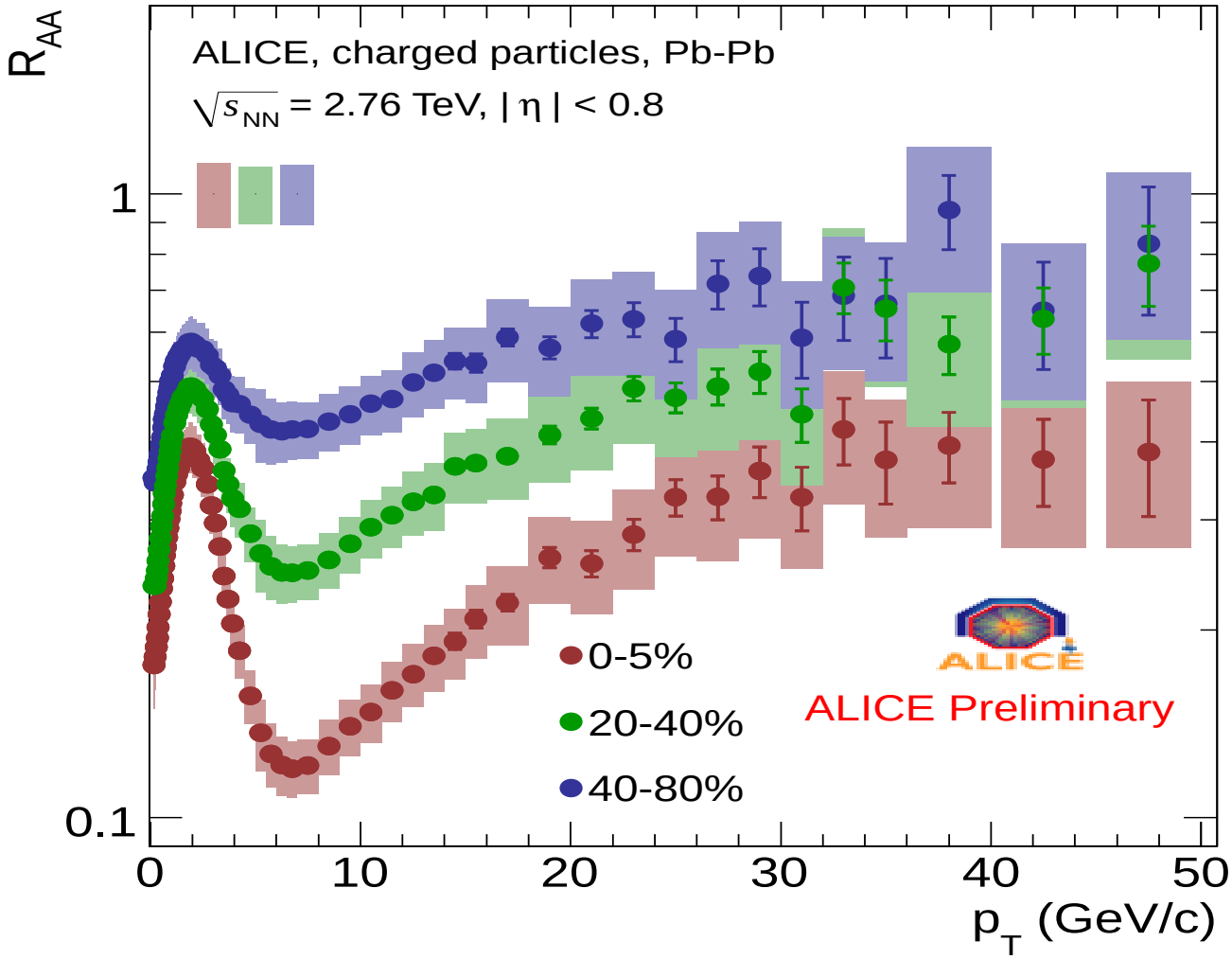

$$R_{AA}(p_T) = \frac{d^2 N^{\pi}_{AA}/dp_T dy N_{AA}}{\langle T_{AA} \rangle d^2 \sigma^{\pi}_{pp}/dp_T dy}$$

Dijet imbalance

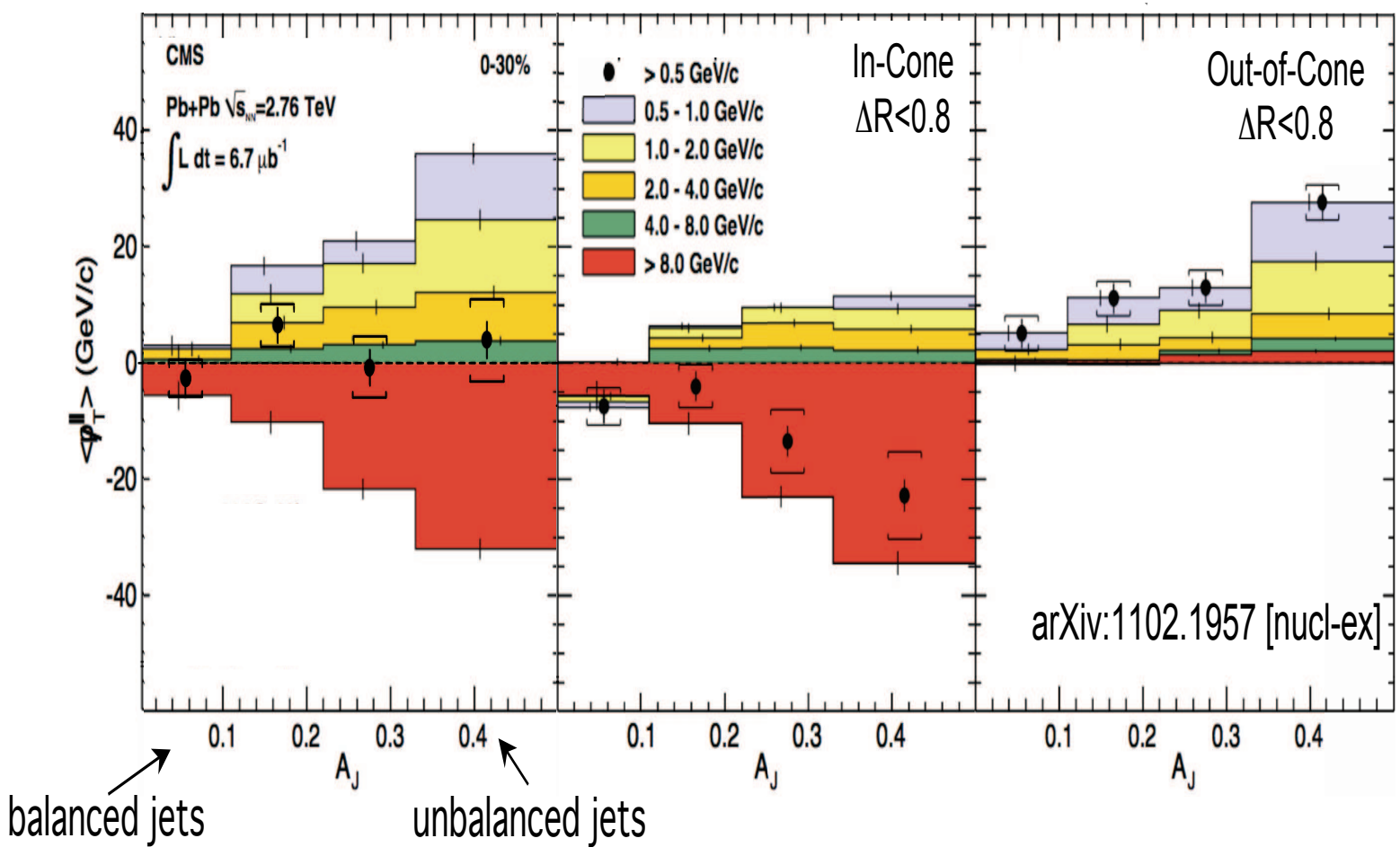

$$\langle p_T^{\parallel} \rangle \quad \text{versus} \quad A_j = \frac{p_{T1} - p_{T2}}{p_{T1} + p_{T2}}$$

Fragmentation functions

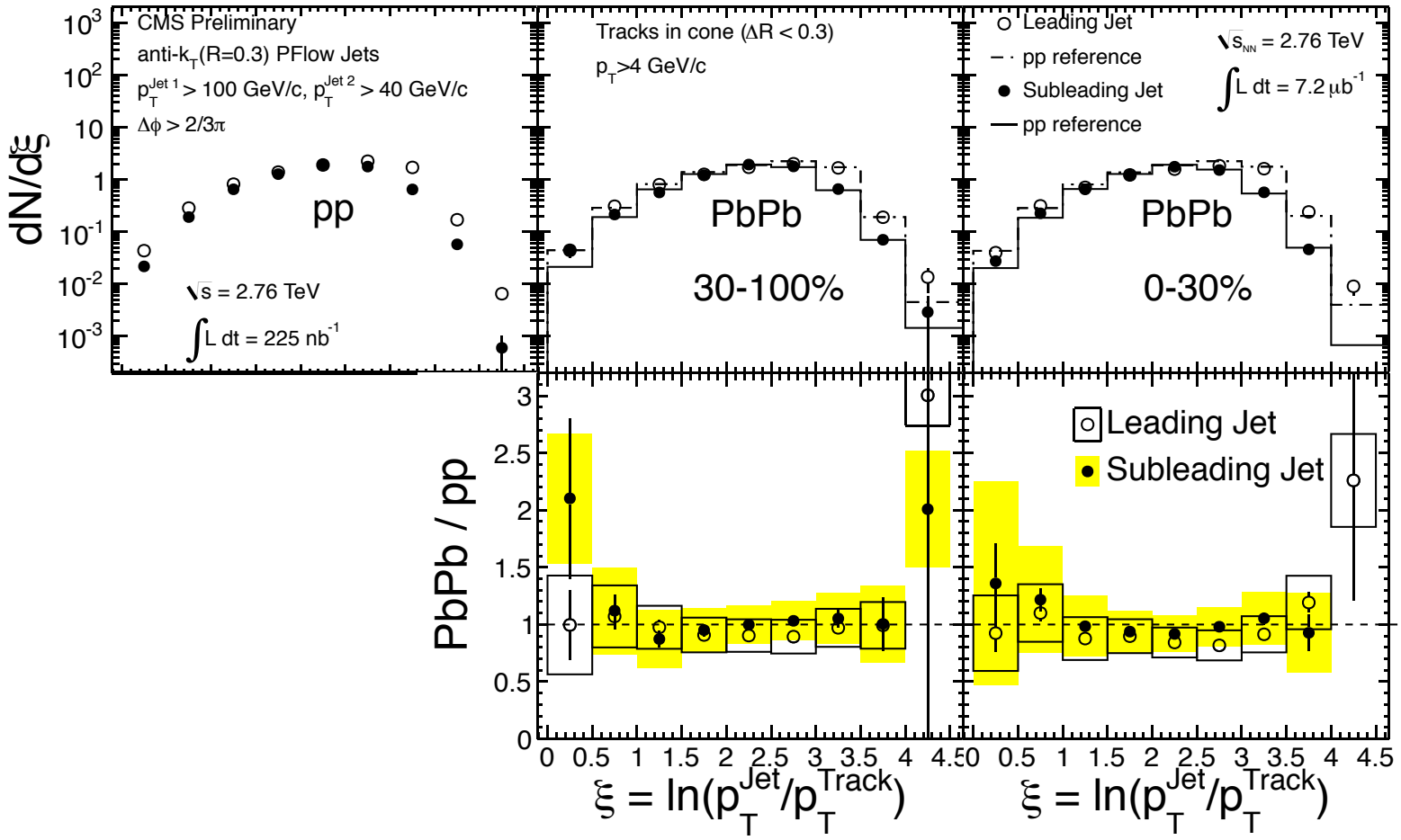

Fragmentation functions

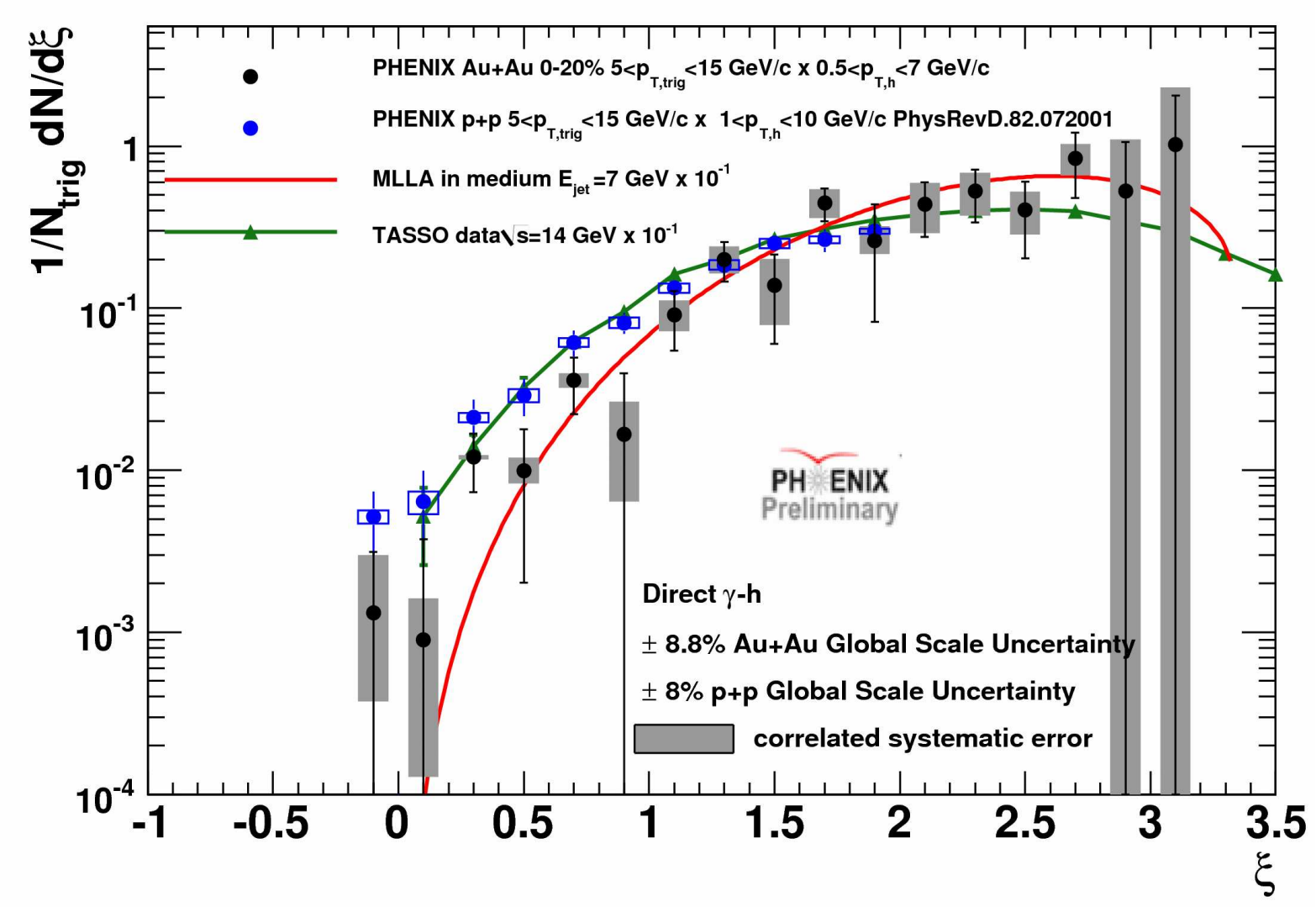

Elliptic flow

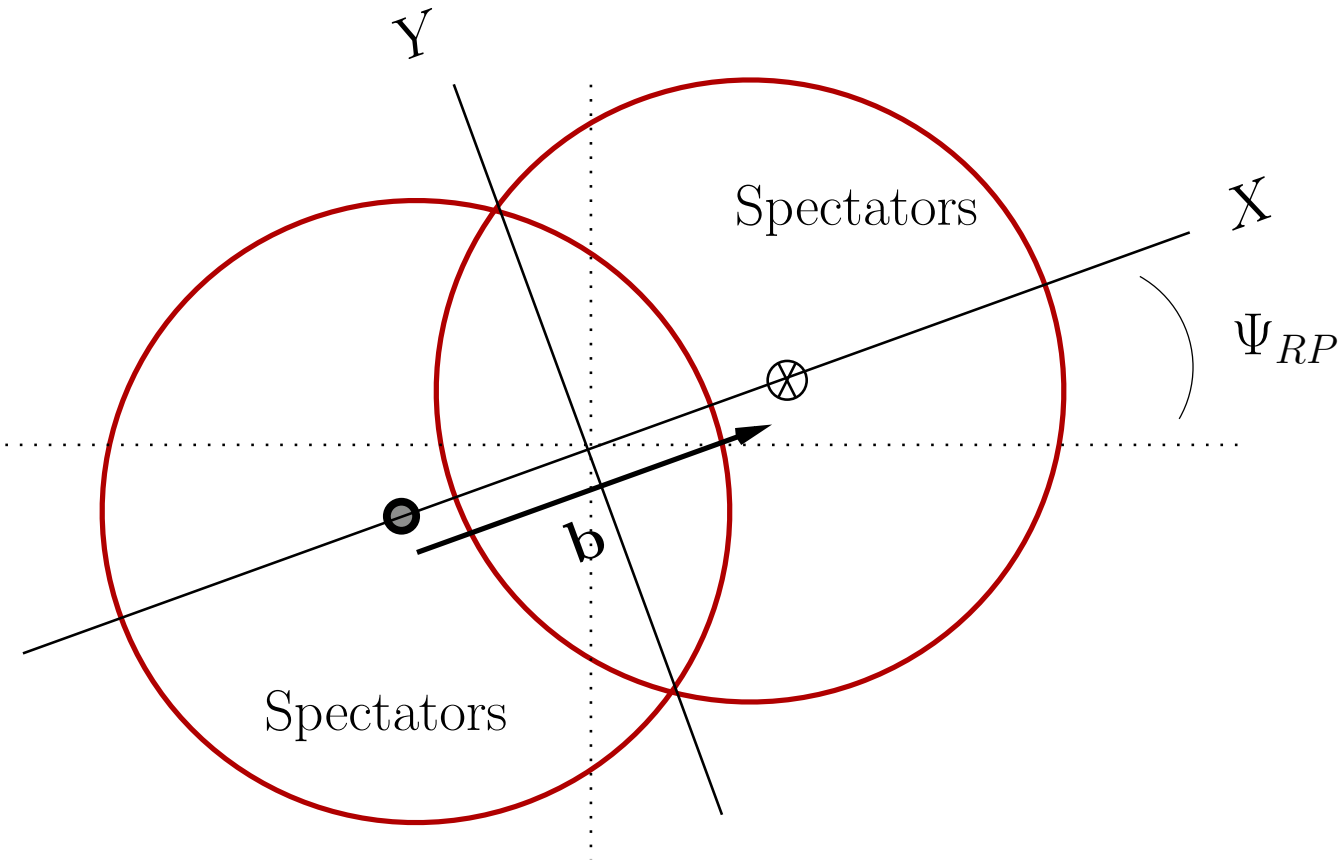

Definition of the reaction plane

Elliptic flow

Spatial asymmetry of the reaction zone

- $$\epsilon_{\mathrm{s,part}} = \frac{\langle y^2 - x^2 \rangle}{\langle y^2 + x^2 \rangle}$$
- $$\langle y^2 - x^2 \rangle = \frac{1}{N_p} \int dx dy \, (y^2 - x^2) \frac{dN_p}{dx \, dy}$$

Momentum asymmetry: elliptic flow

- $$v_2 \equiv \left\langle \frac{p_X^2 - p_Y^2}{p_X^2 + p_Y^2} \right\rangle$$
- $$\frac{1}{p_T} \frac{dN}{dy dp_T d\phi} = \frac{1}{2\pi p_T} \frac{dN}{dy dp_T} (1 + 2v_2(p_T) \cos 2(\phi - \Psi_{RP}) + \ldots)$$

Elliptic flow

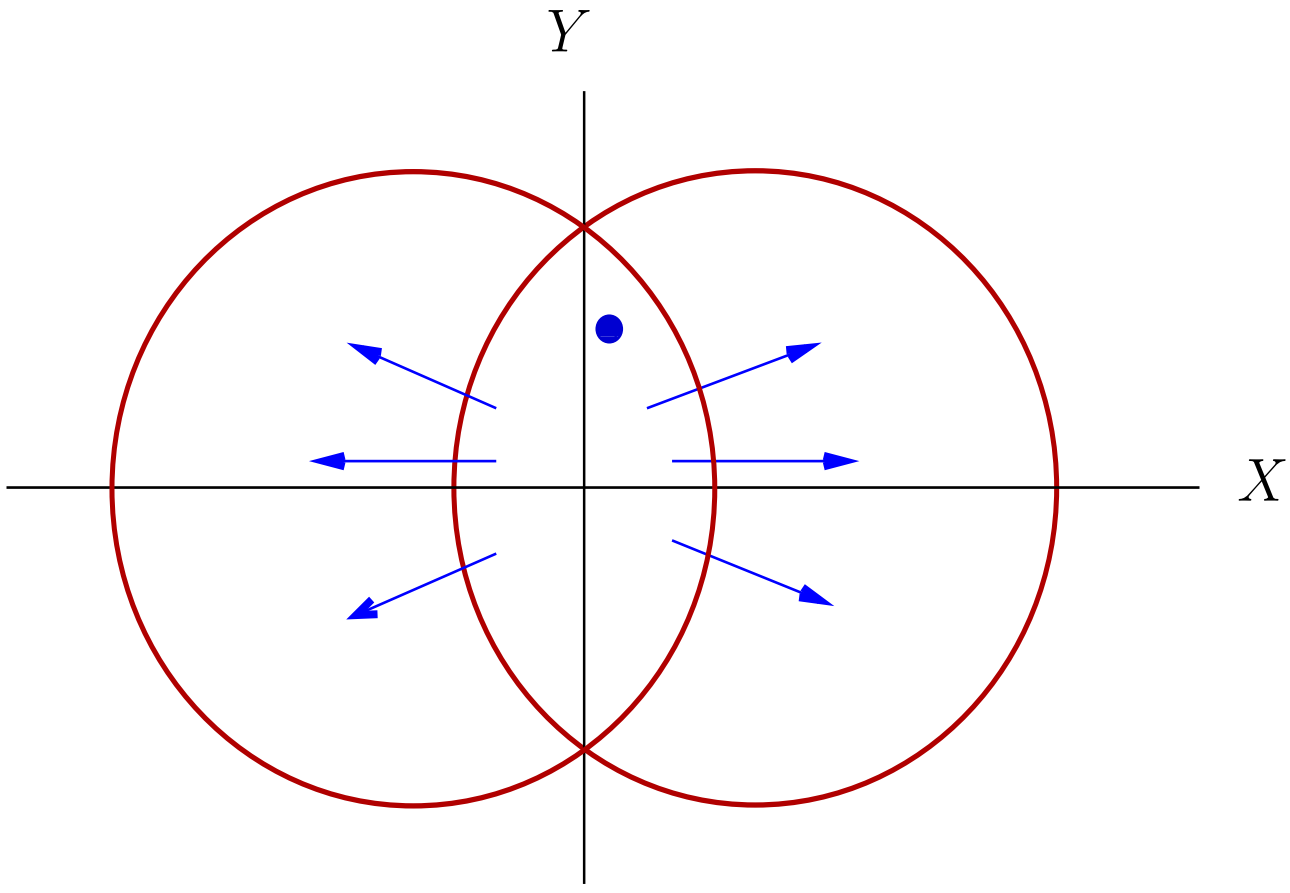

Hydrodynamic origin of the elliptic flow: anisotropic pressure converts spatial anisotropy is into momentum one

Elliptic flow

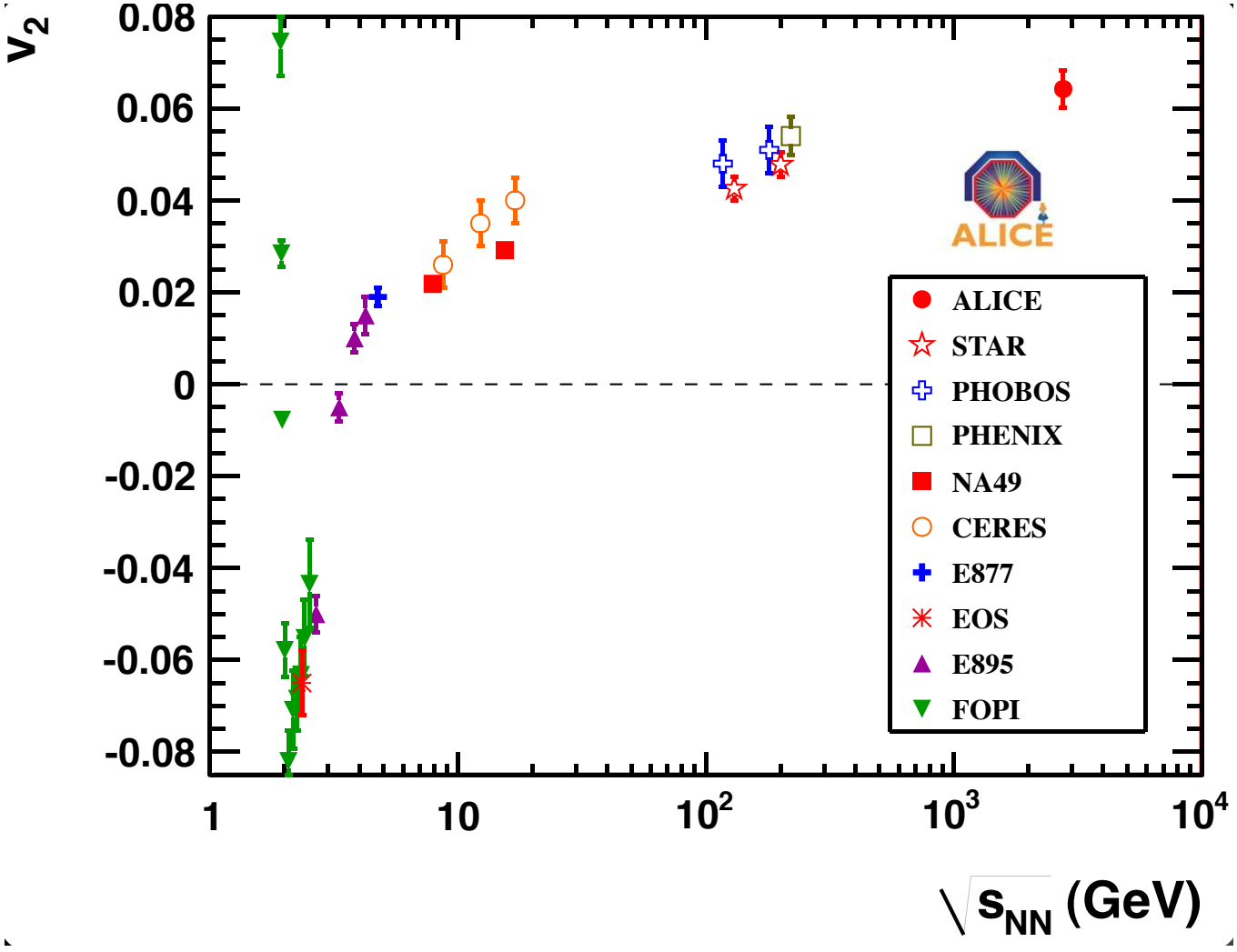

Average elliptic flow as a function of $\sqrt{s}$

Elliptic flow

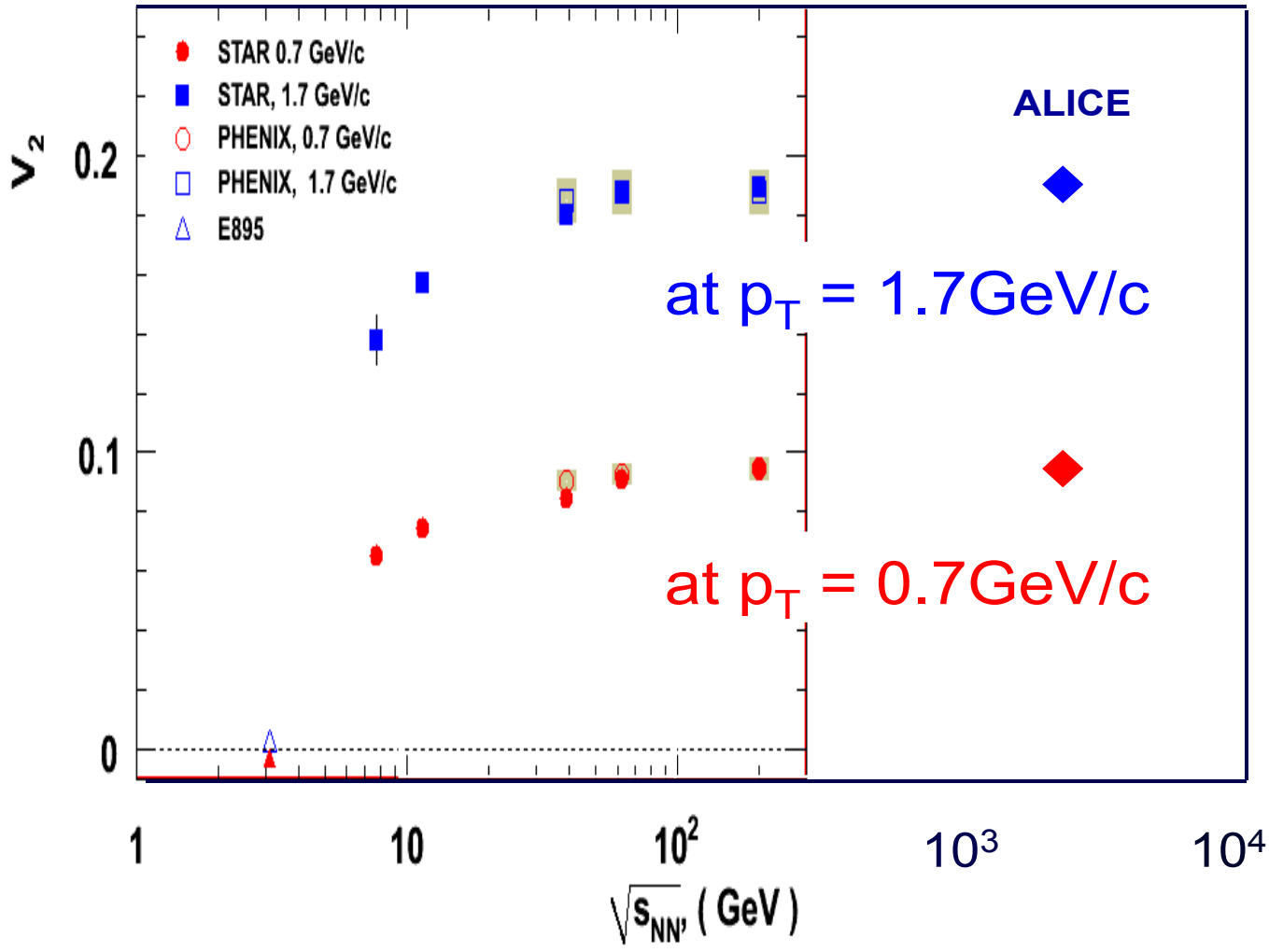

Differential elliptic flow as a function of $\sqrt{s}$

Elliptic flow

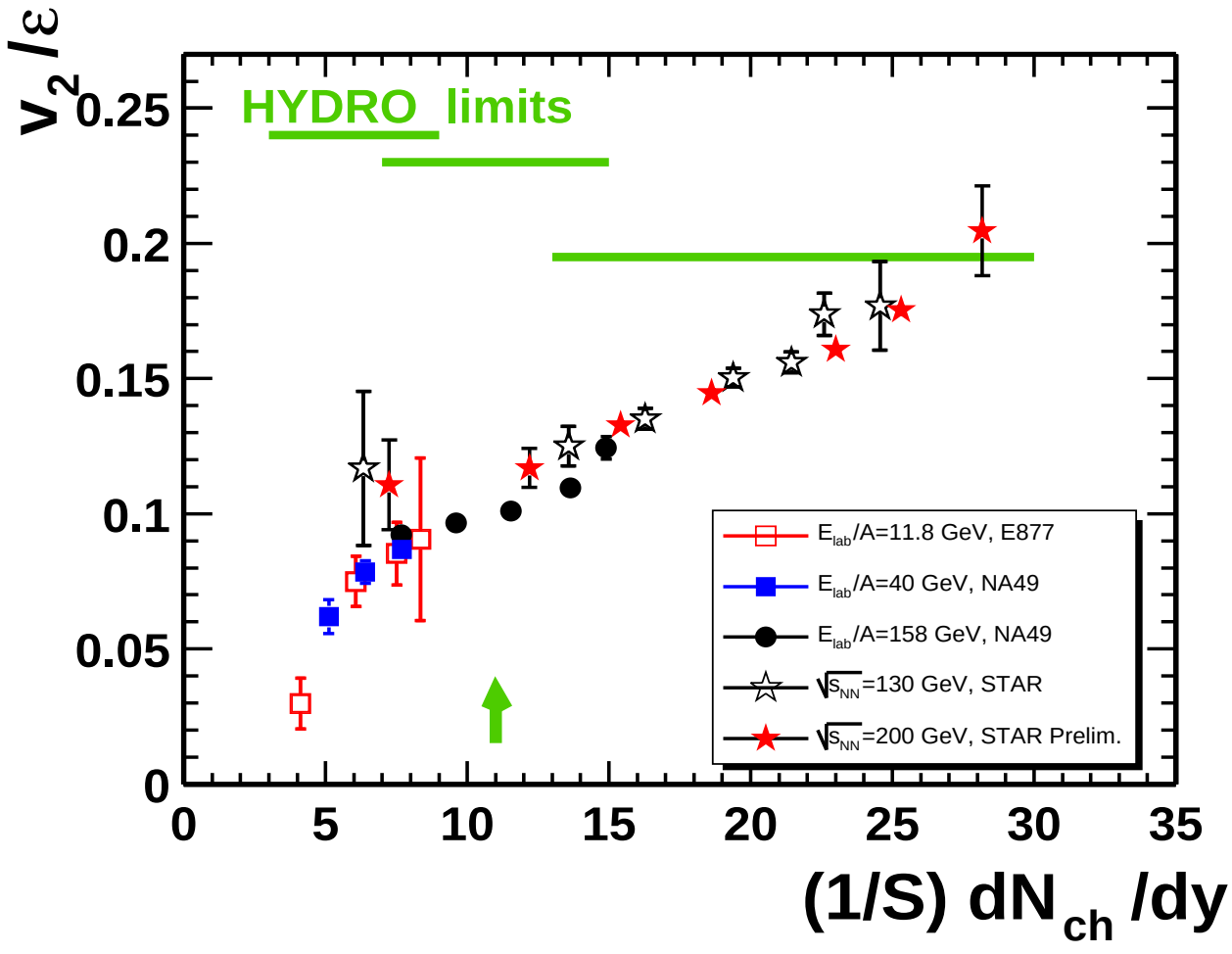

Hydro limit for ideal liquid for v_2 reached at RHIC

Elliptic flow

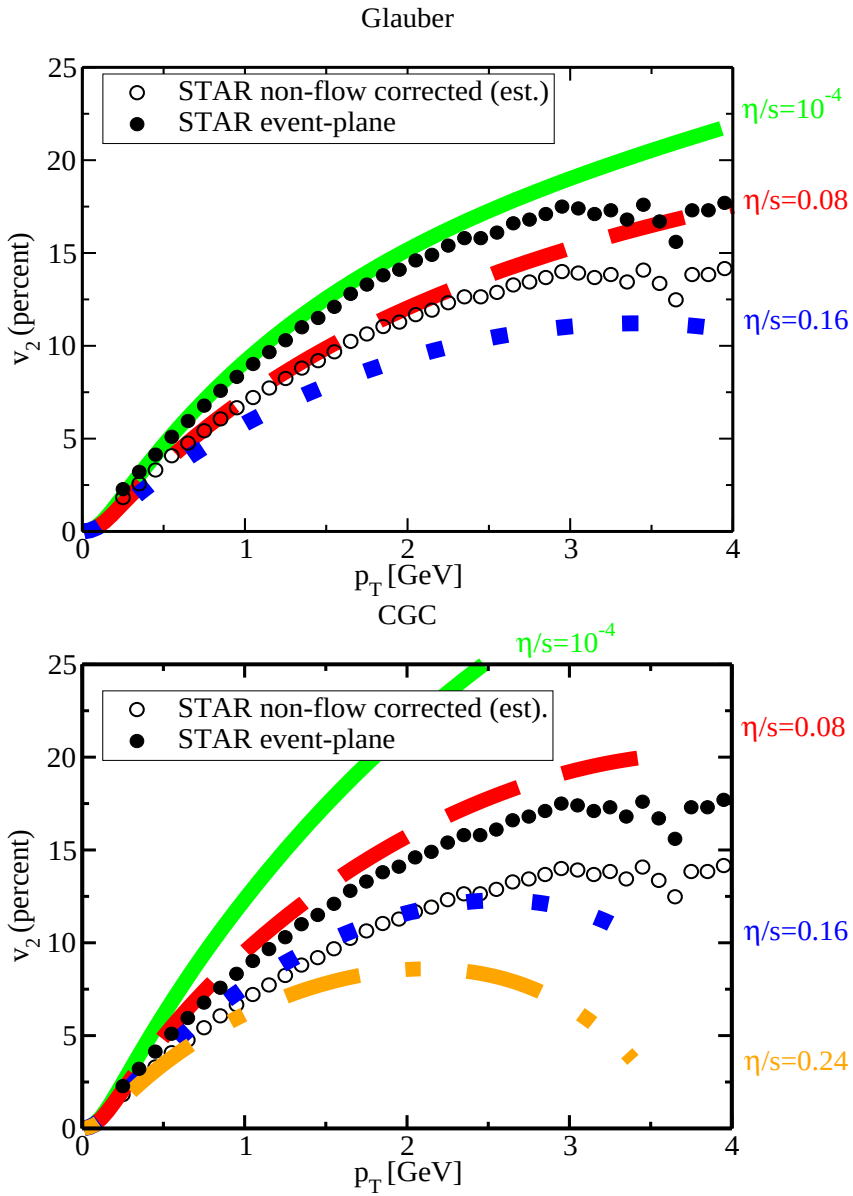

Dependence of v_2 on viscosity for Glauber and CGC initial conditions

Initial conditions

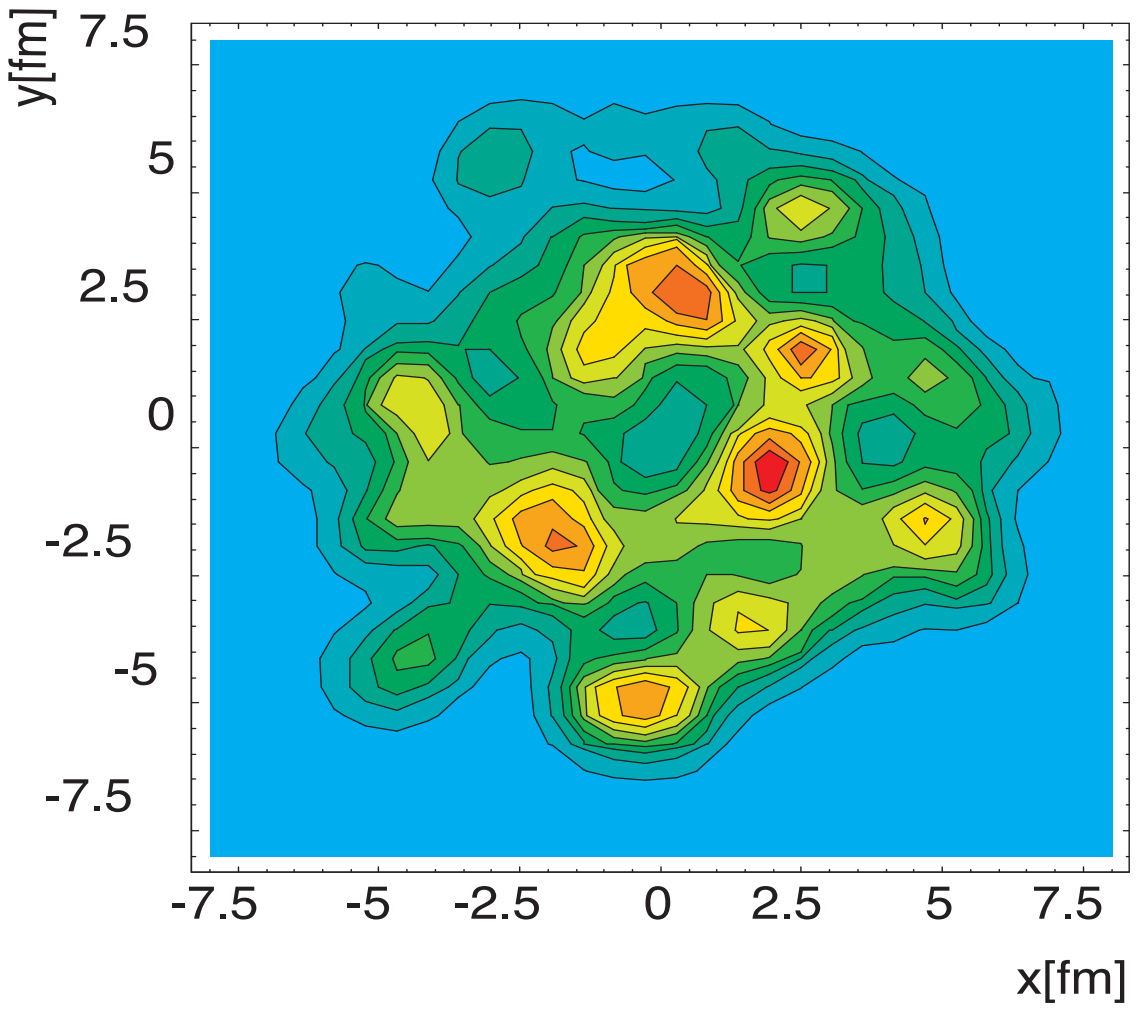

Initial transverse energy density for AuAu collisions at $\sqrt{s} = 200$ GeV

Initial conditions

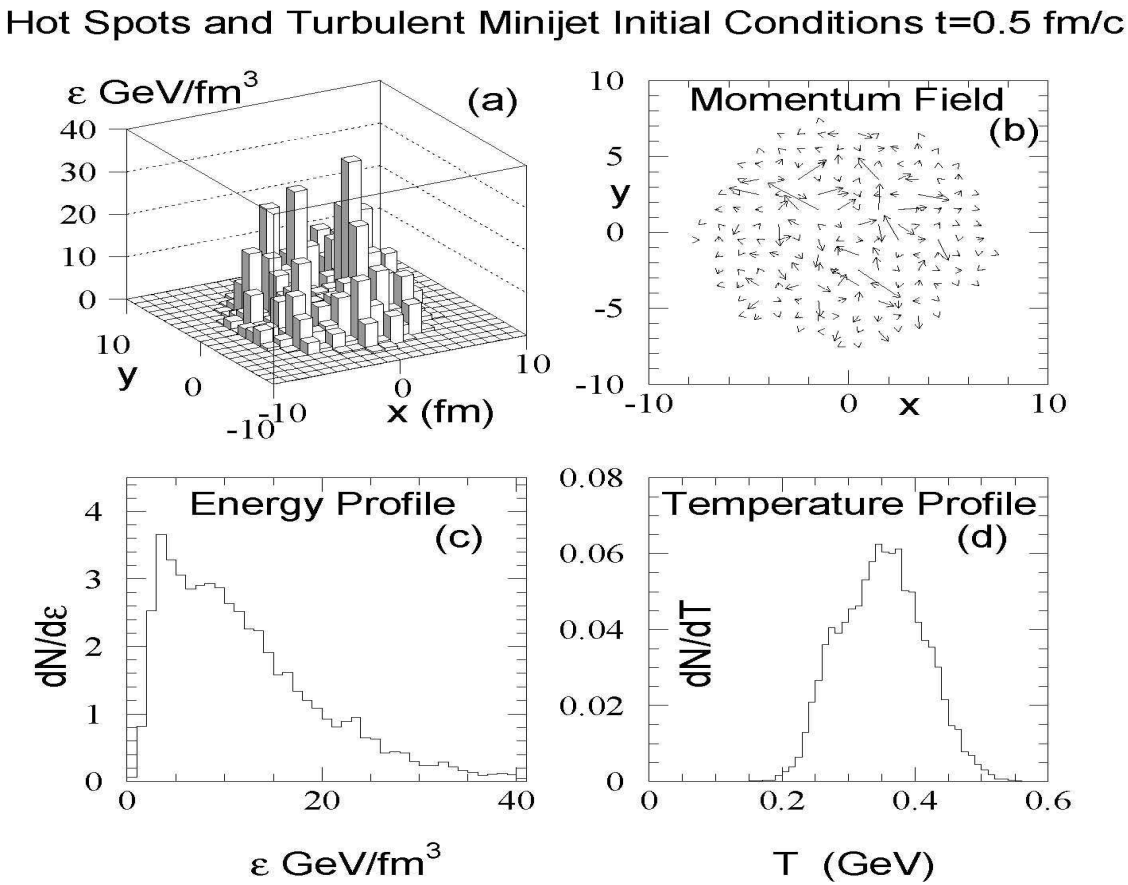

Малый взрыв: перед соударением

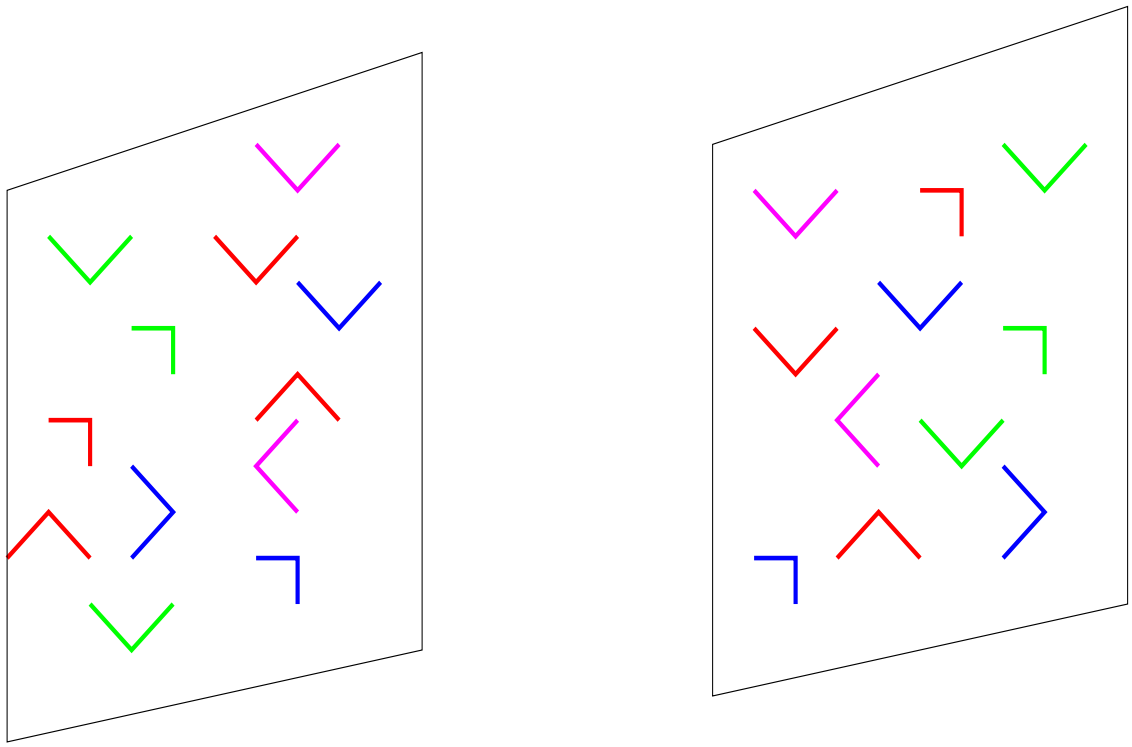

Начальное состояние при $t < 0$

Малый взрыв: стадии соударения

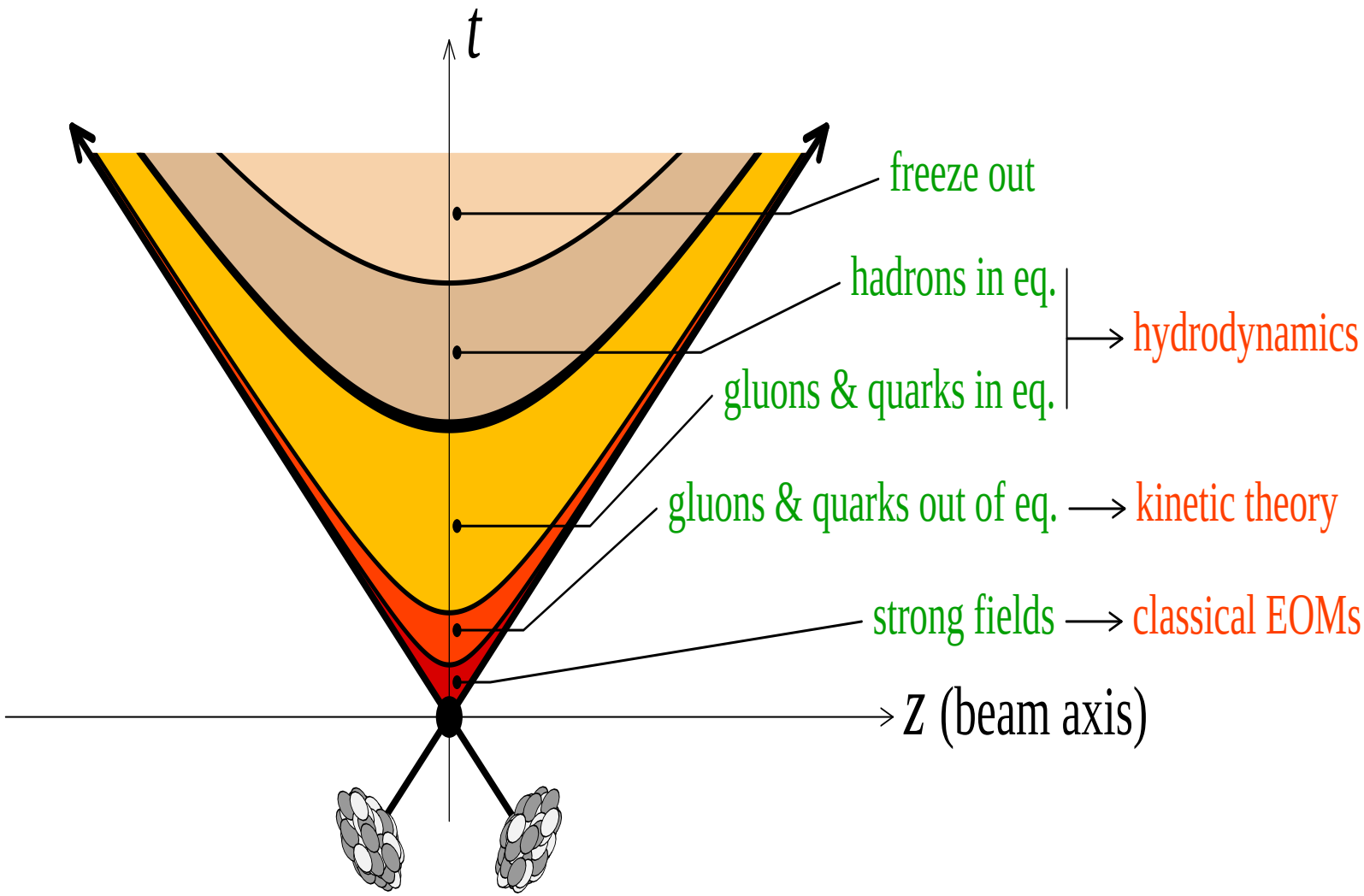

Степени свободы

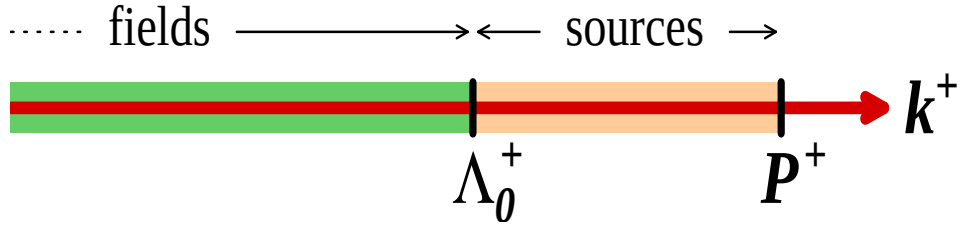

- Характерные времена эволюции для партонных мод

$$\Delta x^+ \sim \frac{1}{k^-} \sim \frac{2k^+}{\mathbf{k}_\perp^2} = \frac{2P^+}{\mathbf{k}_\perp^2} x$$

- Статические моды (источники):

$$x \sim 1$$

- Флуктуационные моды (поля):

$$x \ll 1$$

Физика КХД при высоких энергиях - физика полей с $x \ll 1$

Ядро до соударения: поля

Поля A^a_μ и источник J^a_μ связаны уравнениями

$$[D_\mu, F^{\mu\nu}] = J^\nu \;\Leftrightarrow\; J^\mu = \delta^{\mu+}\rho_1(\mathbf{x}_\perp, x^-)$$

Решение классических уравнений:

$$\begin{aligned} A^+ &= 0, \quad A^- = 0 \\ A^i &= \frac{i}{g} U(\mathbf{x}_\perp, x^-)\partial^i U^\dagger(\mathbf{x}_\perp, x^-) \end{aligned}$$

где

$$\begin{aligned} U(\mathbf{x}_\perp, x^-) &= P\exp\left\{ig\int_{-\infty}^{x^-} dy^-\alpha(\mathbf{x}_\perp, x^-)\right\} \\ \alpha(\mathbf{x}_\perp, x^-) &= -\rho(\mathbf{x}_\perp, x^-)/\nabla^2_\perp \end{aligned}$$

Ядро до соударения: построение наблюдаемых величин

- Зарядовая плотность $\rho(\mathbf{x}_\perp, x^-)$ - случайная величина. Пособытийное усреднение по $\rho(\mathbf{x}_\perp, x^-)$ определяется некоторым функционалом $W_{\Lambda^+}[\rho]$
- Для простейшего случая гауссового ансамбля

$$\langle \rho^a(\mathbf{x}_\perp, x^-)\rho^b(\mathbf{y}_\perp, y^-)\rangle = g^2\mu_A^2\delta^{ab}\delta^2(\mathbf{x}_\perp - \mathbf{y}_\perp)\delta(x^- - y^-))$$

- Структурная функция

$$\begin{aligned} \frac{dN}{d^3k} &= \frac{2k^+}{(2\pi)^3}\langle A_a^i(k, x^+))A_a^i(-k, x^+))\rangle W_{\Lambda^+} \\ \langle A_a^i(0))A_a^i(x))\rangle &\sim \frac{1}{\mathbf{x}_\perp^2}\left(1 - \exp\left[-\mathbf{x}_\perp^2 Q_S^2 \ln(\mathbf{x}_\perp^2\mu^2)\right]\right) \end{aligned}$$

- Q_S^2 - масштаб насыщения,

$$Q_S^2(Y) \simeq Q_0^2 \mathrm{e}^{\lambda_s Y}, \quad Q_0^2 \sim A^{1/3}$$

Ядро до соударения: квантовая эволюция

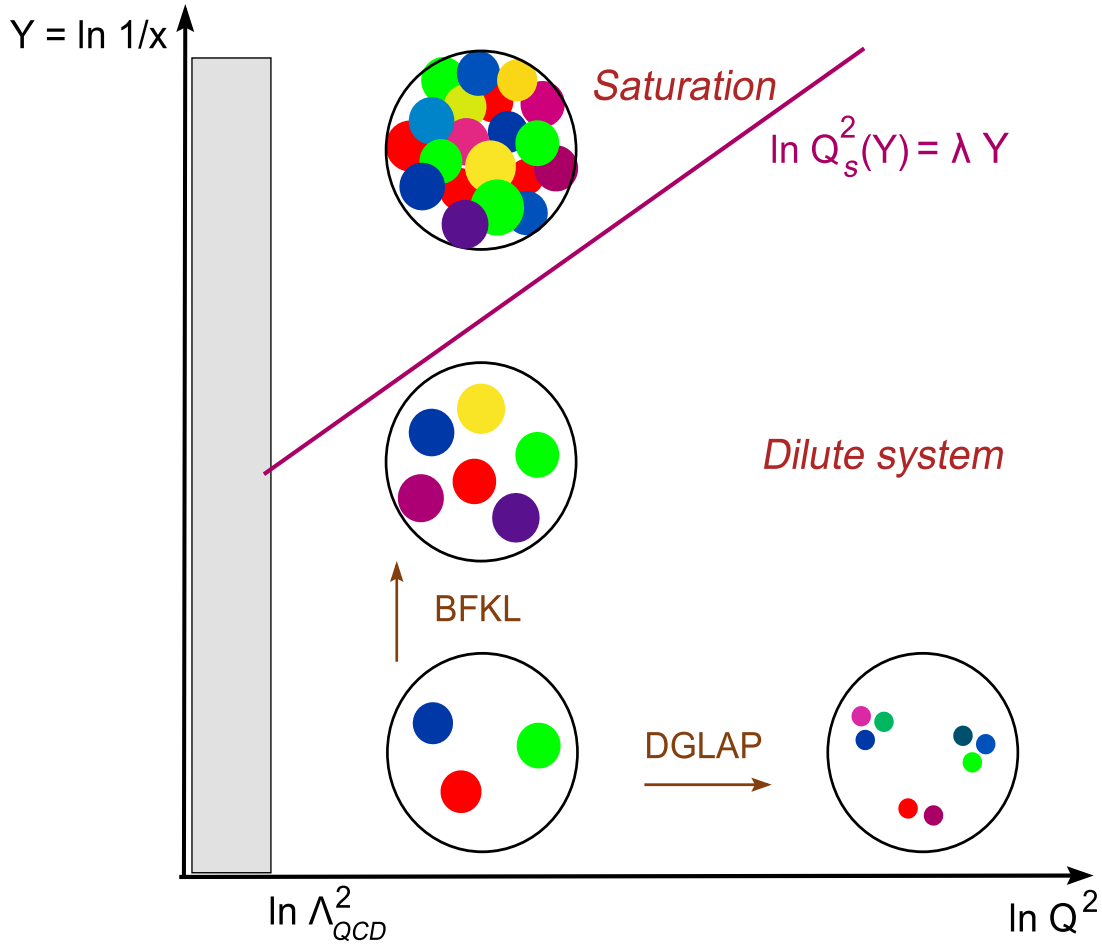

$$x = \frac{k^+}{P^+} \qquad \delta S_\perp \sim \frac{1}{Q^2}$$

Ядро до соударения: квантовая эволюция

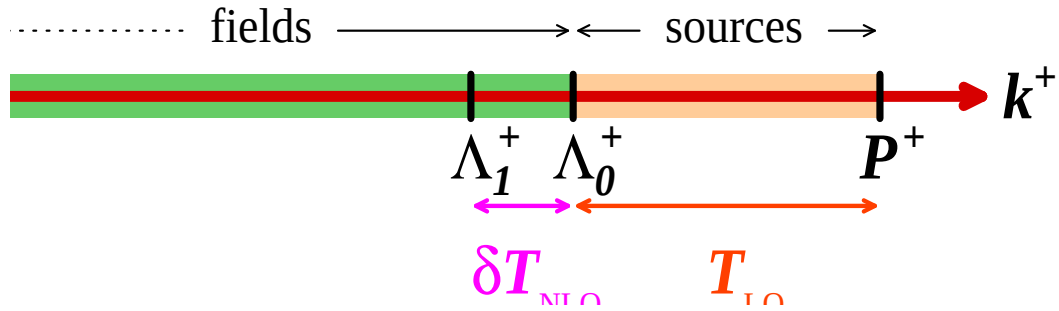

- Структурная функция, классическое приближение

$$< AA >= \int [d\rho]\, W_{\Lambda^+}[\rho]\, A_{\mathrm{cl.}}(\rho)\, A_{\mathrm{cl.}}(\rho)$$

- Произвольная наблюдаемая, классическое приближение

$$\langle \mathcal{O} \rangle_Y = \int [d\alpha] \mathcal{O}[\alpha] W_Y[\alpha]$$

- Квантовая эволюция: уравнение JIMWLK

$$\frac{\partial \langle \mathcal{O}[\alpha] \rangle_Y}{\partial Y} = \langle \frac{1}{2} \int_{x_\perp, y_\perp} \frac{\delta}{\delta \alpha^a_Y(x_\perp)} \chi^{ab}_{x_\perp, y_\perp}[\alpha] \frac{\delta}{\delta \alpha^b_Y(y_\perp)} \mathcal{O}[\alpha] \rangle_Y$$

Ядро до соударения: квантовая эволюция

- Уравнение JIMWLK гамильтоново

$$\frac{\partial \langle \mathcal{O}[\alpha] \rangle_Y}{\partial Y} = \langle \mathcal{H}_{\mathrm{JIMWLK}} \mathcal{O}[\alpha] \rangle_Y$$

- Ядро уравнения JIMWLK

$$\chi^{ab}_{\mathbf{x}_\perp \mathbf{y}_\perp}[\alpha] = \int \frac{d^2\mathbf{z}_\perp}{4\pi^3} \frac{(\mathbf{x}_\perp - \mathbf{z}_\perp)(\mathbf{y}_\perp - \mathbf{z}_\perp)}{(\mathbf{x}_\perp - \mathbf{z}_\perp)^2 (\mathbf{y}_\perp - \mathbf{z}_\perp)^2} \left[\left(1 - U^\dagger_{\mathbf{x}_\perp} U_{\mathbf{z}_\perp}\right) \left(1 - U^\dagger_{\mathbf{z}_\perp} U_{\mathbf{y}_\perp}\right) \right]$$

- Нелинейная зависимость от источников

$$U^\dagger(\mathbf{x}_\perp, x^-) = P \exp\left\{ ig \int_{-\infty}^{x^-} dy^- \alpha^a(\mathbf{x}_\perp, x^-) T^a \right\}$$

- В пределе малых α JIMWLK переходит в BFKL

Соударение ядер: классическое решение

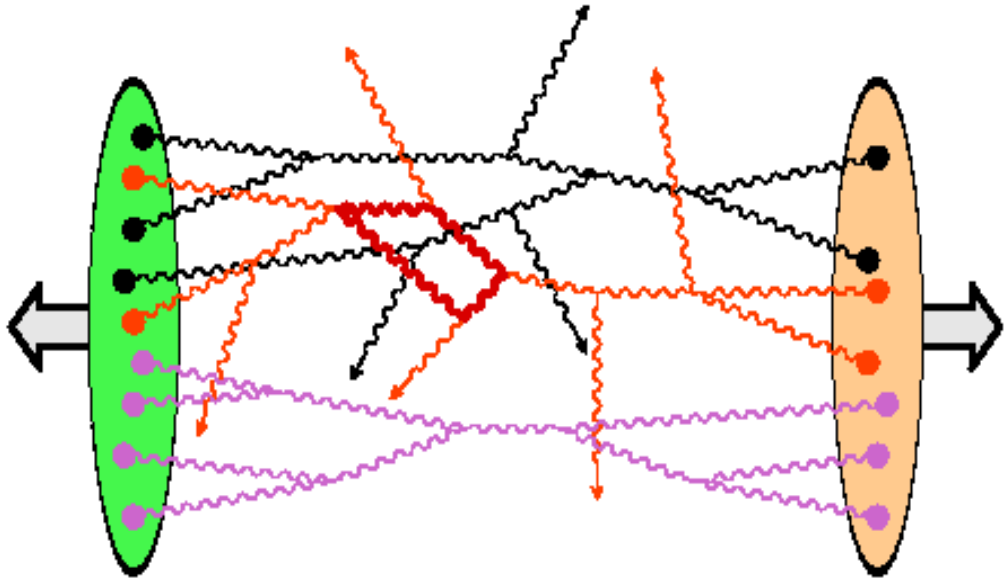

$$[D_\mu, F^{\mu\nu}] = J^\nu$$

$$J^\mu = \delta^{\mu+}\rho_1(\mathbf{x}_\perp, x^-) + \delta^{\mu+}\rho_2(\mathbf{x}_\perp, x^-)$$

Ищем решение во всех порядках по источникам $\rho_{1,2}$

Буст-инвариантное классическое решение

- Координаты τ, η

$$x^0 + x^3 = \tau \mathrm{e}^{\eta}, \qquad x^0 - x^3 = \tau \mathrm{e}^{-\eta}$$

- Для одного источника использовались калибровки $A^{\pm} = 0$
- Для задачи с двумя источниками удобно использовать калибровку $A^{\tau} = 0$

$$A_{\tau} = A^{\tau} \equiv \frac{1}{\tau}(x^+ A^- + x^- A^+)$$

- Буст-инвариантное решение не зависит от быстроты η

Буст-инвариантное классическое решение

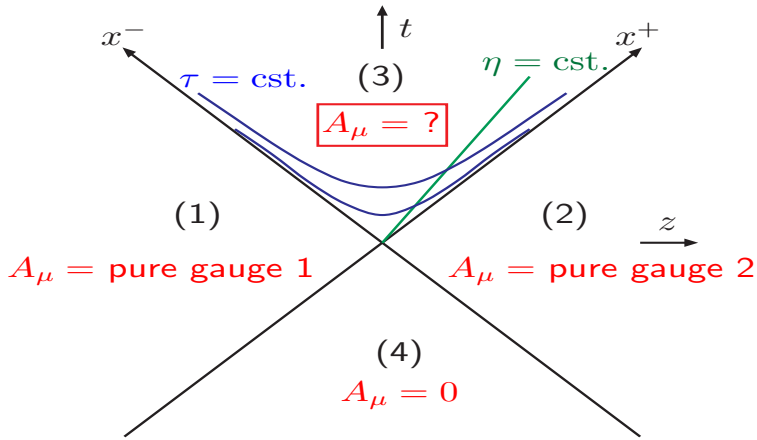

- Ищем решение (не зависящее от η !) в виде:

$$A^i = \theta(-x^+)\theta(x^-)A^i_{(1)} + \theta(x^+)\theta(-x^-)A^i_{(2)} + \theta(x^+)\theta(x^-)A^i_{(3)}$$
$$A^\eta = \theta(x^+)\theta(x^-)A^\eta_{(3)}$$

- Условие согласования при $\tau = 0$:

$$A^i_{(3)}|_{\tau=0} = A^i_{(1)} + A^i_{(2)}$$
$$A^\eta_{(3)}|_{\tau=0} = \frac{ig}{2}\left[A^i_{(1)}, A^i_{(2)}\right]$$

Непосредственно после соударения генерируются продольные электрические и магнитные поля - глазма :

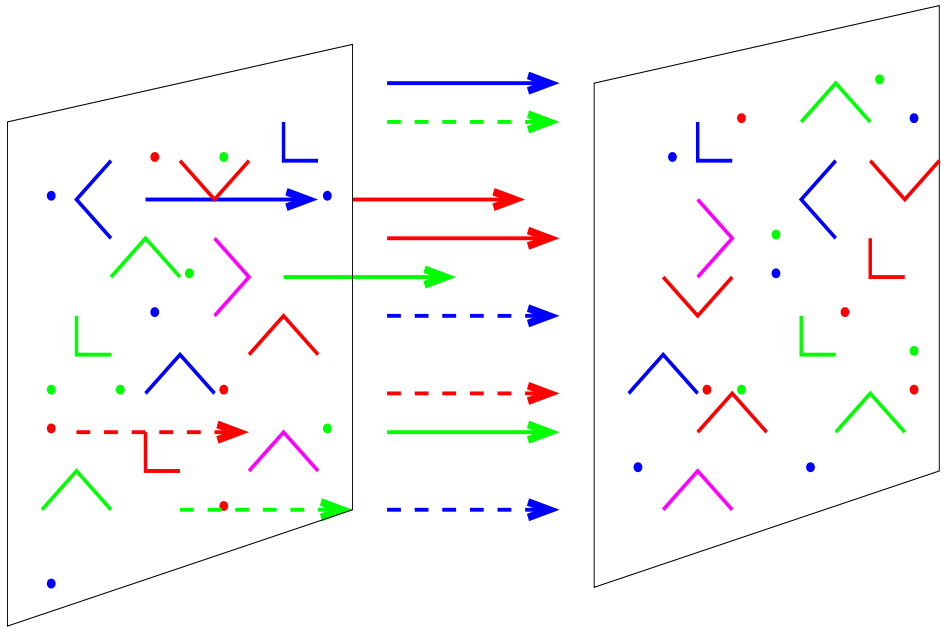

$$E^z = ig\left[A^i_{(1)}, A^i_{(2)}\right]$$

$$B^z = ig\epsilon^{ij}\left[A^i_{(1)}, A^j_{(2)}\right]$$

Временная эволюция продольных и поперечных полей:

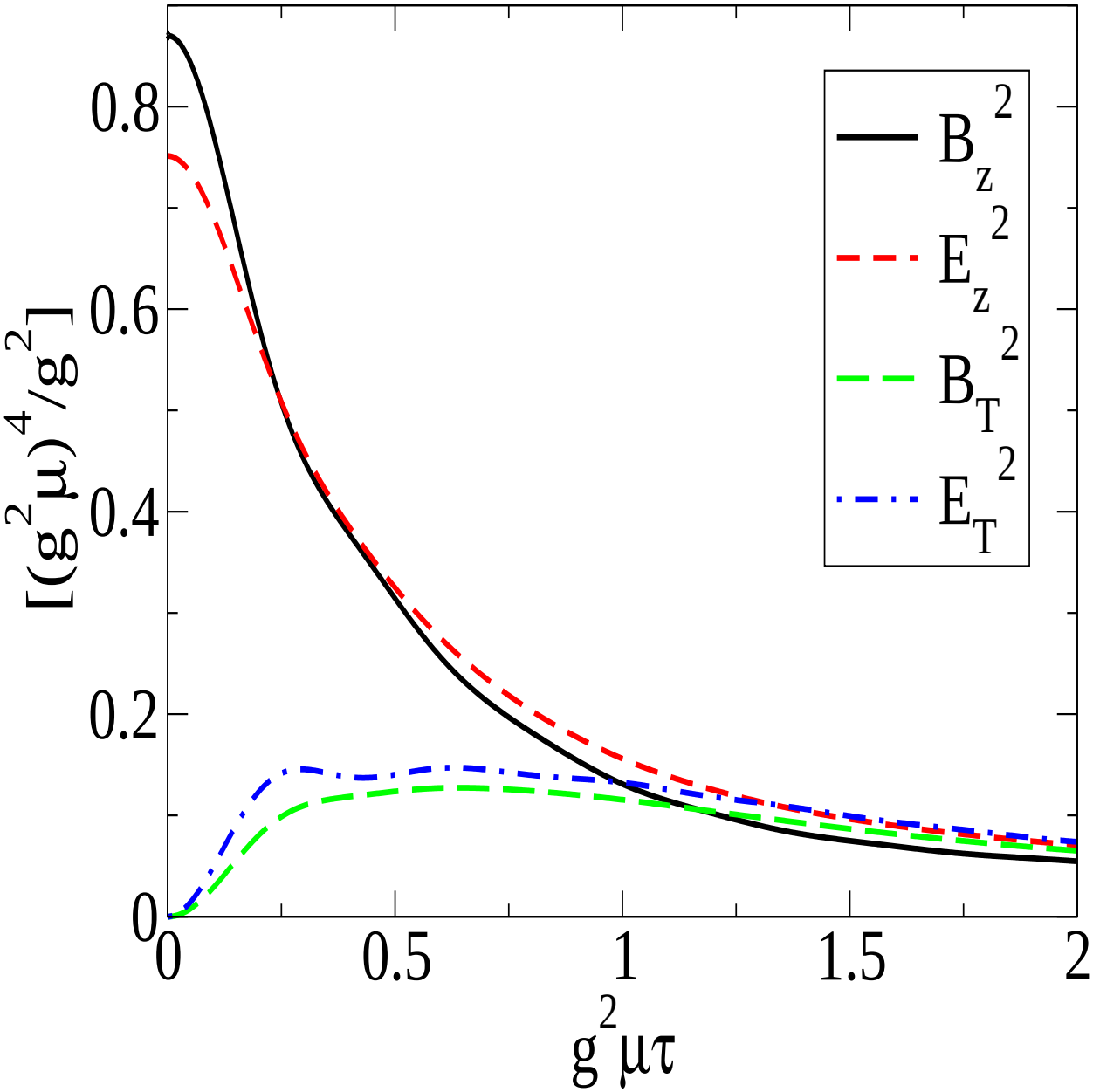

Начальные условия: гидродинамика

- Уравнения движения

$$\partial_\mu T^{\mu\nu} = 0$$

- Уравнение состояния

$$p = f(\epsilon)$$

- Начальные условия задаются при некотором $\tau = \tau_0$

$$T^{\mu\nu}(\tau = \tau_0, \eta, \mathbf{x}_\perp)$$

- Общая структура $T^{\mu\nu}$:

$$T^{\mu\nu} = \begin{pmatrix} \epsilon & & & \\ & \frac{\epsilon}{3} & & \\ & & \frac{\epsilon}{3} & \\ & & & \frac{\epsilon}{3} \end{pmatrix}$$

Начальные условия: конденсат цветного стекла

Для конфигурации $\mathbf{E}^a_\mu = \lambda \mathbf{B}^a_\mu$

$$\langle T^{\mu\nu}(\tau = 0^+, \eta, \mathbf{x}_\perp)\rangle = \begin{pmatrix} \epsilon & & & \\ & \epsilon & & \\ & & \epsilon & \\ & & & -\epsilon \end{pmatrix}$$

Очень не похоже на гидродинамику, но очень похоже на струнные модели в КХД (отрицательное p_z !)

глазменные трубки	струны
отрицательное p_z	натяжение струны
глазменные неустойчивости	разрыв струны

Механизм изотропизации?

Начальные условия: конденсат цветного стекла

- $$\frac{dN}{d\eta}|_{\eta=0} = c_N \frac{\pi R_A^2 Q_S^2}{\alpha_s}$$
- $$\frac{dE_\perp}{d\eta}|_{\eta=0} = c_E \frac{\pi R_A^2 Q_S^3}{\alpha_s}$$

$$\mathrm{HERA} \Rightarrow Q_S^2 \simeq 1.2\,\mathrm{GeV} \Rightarrow \frac{dN}{d\eta}|_{\eta=0} \simeq 1100$$

Глазменная неустойчивость

- Рассмотрим возмущения, зависящие от быстроты η:

$$E_i(0,\eta,\mathbf{x}_\perp) = \delta E_i(\eta,\mathbf{x}_\perp)\ ,$$
$$E_\eta(0,\eta,\mathbf{x}_\perp) = i\,g\,[\alpha_1^i,\alpha_2^i] + \delta E_\eta(\eta,\mathbf{x}_\perp,)\ ,$$

- Максимальная фурье-компонента среднего продольного давления $P_L = \tau^2 T^{\eta\eta}$

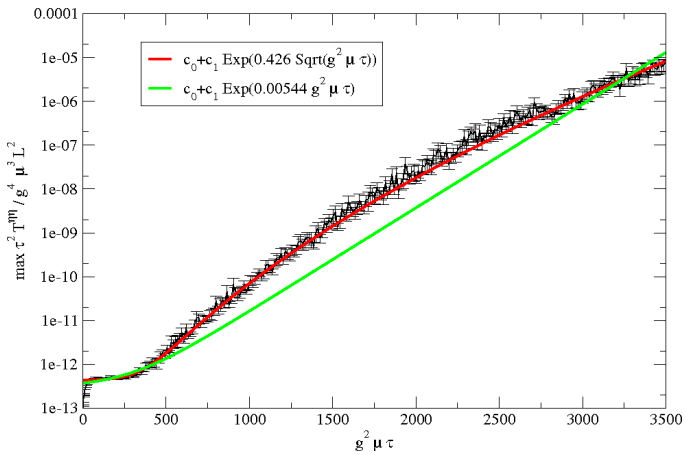

- Отклонения от буст-инвариантности генерируют экспоненциально растущие поперечные поля

$$|E_\perp|, |B_\perp| \sim \mathrm{e}^{\sqrt{Q_s \tau}}$$

Начальные условия: квантовая эволюция. Факторизация

- В ведущем порядке

$$T^{\mu\nu}_{\mathrm{LO}} = \frac{1}{4} g^{\mu\nu} F^{\lambda\sigma} F_{\lambda\sigma} - F^{\mu\lambda} F^{\nu}_{\lambda}$$

$$[F_\mu, F^{\mu\nu}] = J^\nu, \qquad \lim_{t\to-\infty} A^\mu(t, \mathbf{x}) = 0$$

- Квантовые поправки

$$\delta T^{\mu\nu}_{\mathrm{NLO}} = \left[\ln\left(\frac{\Lambda_0^+}{\Lambda_1^+}\right) \mathcal{H}_1 + \ln\left(\frac{\Lambda_0^-}{\Lambda_1^-}\right) \mathcal{H}_2 \right] T^{\mu\nu}_{\mathrm{LO}}$$

- Квантовые поправки можно отнести к эволюции матрицы плотности

$$\langle T^{\mu\nu}_{\mathrm{LO}} + \delta T^{\mu\nu}_{\mathrm{NLO}} \rangle = \langle T^{\mu\nu}_{\mathrm{LO}} \rangle_{\Lambda_1}$$

- Новое усреднение идет с матрицей плотности

$$W_{\Lambda_1^\pm} = \left[1 + \ln\left(\frac{\Lambda_0^\pm}{\Lambda_1^\pm}\right) \mathcal{H}_{1,2} \right] W_{\Lambda_0^\pm}$$

Начальные условия: квантовая эволюция. Факторизация

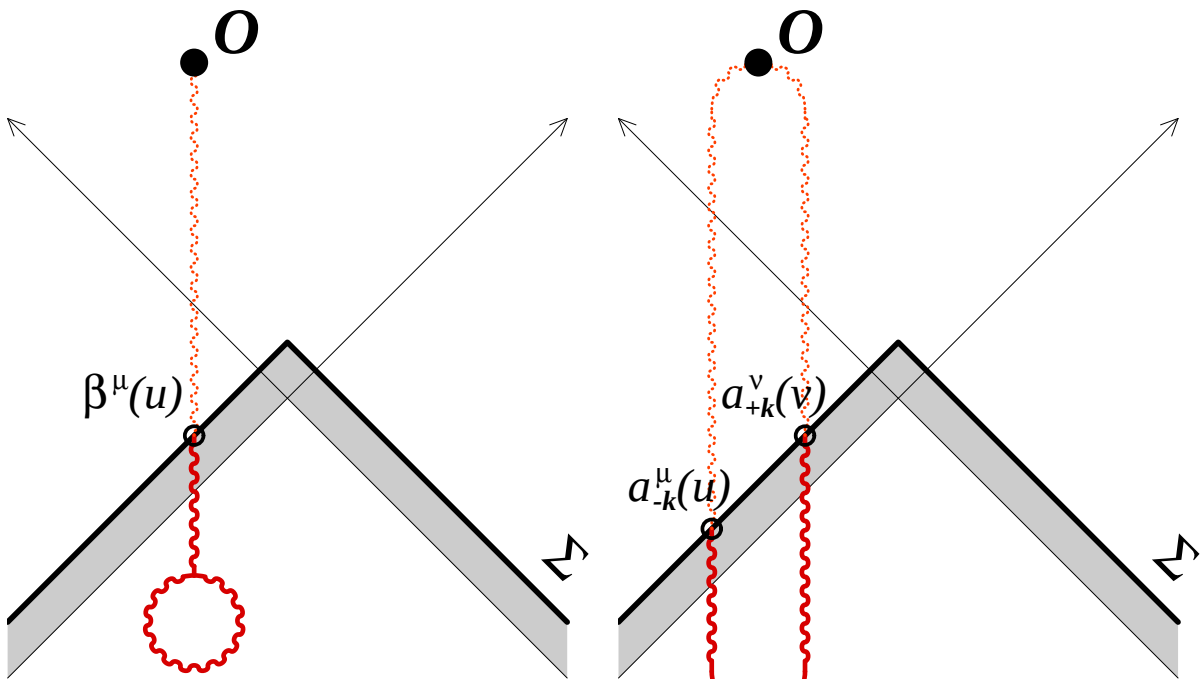

- Общая структура квантовых поправок

$$\langle O\rangle_{\mathrm{NLO}} = \left[\frac{1}{2}\int_{\Sigma} \mathrm{d}^3\mathbf{u}\mathrm{d}^3\mathbf{v}\mathcal{G}_{\mu\nu}(\mathbf{u},\mathbf{v})\mathbb{T}^{\mu}_{\mathbf{u}}\mathbb{T}^{\nu}_{\mathbf{v}} + \int_{\Sigma}\mathrm{d}^3\mathbf{u}\beta_{\mu}(\mathbf{u})\mathbb{T}^{\nu}_{\mathbf{u}}\right]\langle O\rangle_{\mathrm{LO}}.$$

- $\mathbb{T}_{\mathbf{u}}$ - производная Ли по начальной конфигурации!

$$a^{\mu}(x) = \int_{\vec{\mathbf{u}}\in\Sigma} a(\vec{\mathbf{u}})\cdot\mathbb{T}_{\mathbf{u}}\mathcal{A}^{\mu}(x)$$

Пример: одноинклюзивное сечение

- Общая формула

$$\frac{dN}{d^3\mathbf{p}} \sim \sum_{n=0}^{\infty} \frac{1}{n!} \int \left[d^3\mathbf{p}_1 \cdots d^3\mathbf{p}_n \right] \left| \left\langle \mathbf{p}\ \mathbf{p}_1 \cdots \mathbf{p}_n \middle| 0 \right\rangle \right|^2 .$$

- Древесное приближение

$$\frac{dN_{\mathrm{LO}}}{d^3\mathbf{p}} = \int d^3\mathbf{x} d^3\mathbf{y}\ e^{i\mathbf{p}\cdot(\mathbf{x}-\mathbf{y})}\ (\cdots) \Big[\mathcal{A}^{\mu}(t,\mathbf{x}) \mathcal{A}^{\nu}(t,\mathbf{y}) \Big] \Big|_{t\to\infty} .$$

- Квантовые поправки

$$\begin{aligned} \frac{dN_{\mathrm{NLO}}}{d^3\mathbf{p}} \quad = \quad & \lim_{t\to\infty} \int_{\mathbf{x},\mathbf{y}} e^{i\mathbf{p}\cdot(\mathbf{x}-\mathbf{y})}\ (\cdots) \\ & \Big[\mathcal{G}^{\mu\nu}_{+-}(x,y) + \beta^{\mu}_{+}(t,\mathbf{x})\ \mathcal{A}^{\nu}_{-}(t,\mathbf{y}) + \mathcal{A}^{\mu}_{+}(t,\mathbf{x})\ \beta^{\nu}_{-}(t,\mathbf{y}) \Big] \Big| . \end{aligned}$$

Глазменные нестабильности: ресуммирование

- Ресуммирование

$$\langle O\rangle_{\rm res} = \exp\left[\frac{1}{2}\int_\Sigma \mathrm{d}^3\mathbf{u}\mathrm{d}^3\mathbf{v}\mathcal{G}_{\mu\nu}(\mathbf{u},\mathbf{v})\mathbb{T}^\mu_{\mathbf{u}}\mathbb{T}^\nu_{\mathbf{v}} + \int_\Sigma \mathrm{d}^3\mathbf{u}\beta_\mu(\mathbf{u})\mathbb{T}^\nu_{\mathbf{u}}\right]\langle O\rangle_{\rm LO}$$

- Полезное тождество

$$\exp\left[\frac{1}{2}\int_\Sigma \alpha(\mathbf{u})\mathbb{T}_{\mathbf{u}}\right]\langle O\rangle_{\rm LO}[\phi_0] = O[\phi_0+\alpha]$$

- Тем самым, предложенное ресуммирование эквивалентно усреднению по гауссовым флуктуациям начальной полевой конфигурации

$$O_{\rm res} = \exp\left[\frac{1}{2}\int_\Sigma \mathrm{d}^3\mathbf{u}\mathrm{d}^3\mathbf{v}\mathcal{G}(\mathbf{u},\mathbf{v})\mathbb{T}_{\mathbf{u}}\mathbb{T}_{\mathbf{v}} + \int_\Sigma \mathrm{d}^3\mathbf{u}\beta(\mathbf{u})\mathbb{T}_{\mathbf{u}}\right] O_{\rm LO}[\phi_0]$$

$$= \int \mathcal{D}\alpha \exp\left[-\frac{1}{2}\int_\Sigma \mathrm{d}^3\mathbf{u}\mathrm{d}^3\mathbf{v}\alpha(\mathbf{u})\mathcal{G}^{-1}(\mathbf{u},\mathbf{v})\alpha(\mathbf{v})\right] O[\phi_0+\alpha+\beta]$$

Particle production at strong coupling: e^+e^- annihilation

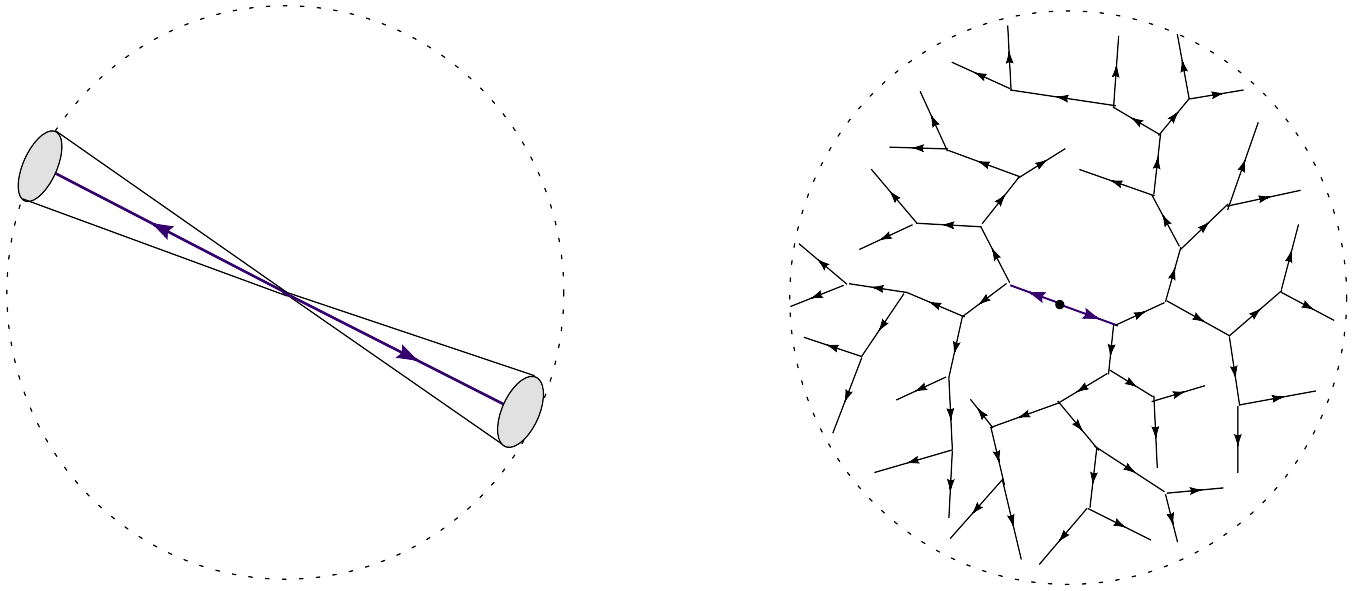

- Left: particle production in the weak coupling regime.
- Right: particle production in the strong coupling regime.

Shock wave collision in the bulk: trapped surface

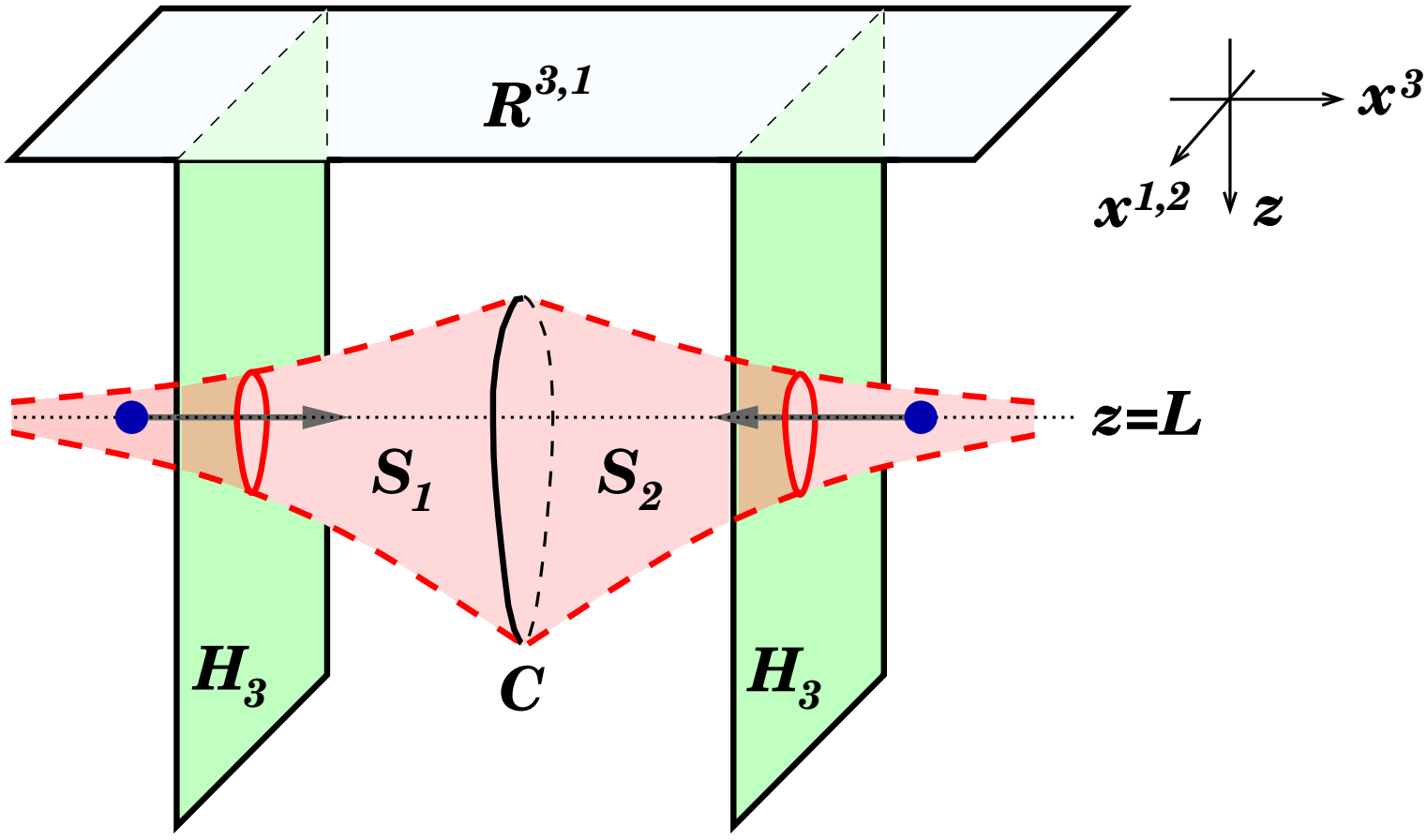

Here C is a two-sphere

Shock wave collision in the bulk: scattering of shock waves

- Line element for head-on collision of gravitational shock waves:

$$\begin{aligned} ds^2 &= \frac{L^2}{z^2}\left[-dudv + (dx^1)^2 + (dx^2)^2 + dz^2\right] \\ &+ \frac{L}{z}\Phi(x^1, x^2, z)\left[\delta(u)du^2 + \delta(v)dv^2\right] \end{aligned}$$

where $u = t - x^3$ and $v = t + x^3$

- Simplest case: particle as a boosted black hole:

$$\begin{aligned} \Phi(x^1, x^2, z) &= \frac{2G_5 E}{L}\left[\frac{1 + 8q(1+q) - 4\sqrt{q(1+q)}(1+2q)}{\sqrt{q(1+q)}}\right] \\ q &\equiv \frac{(x^1)^2 + (x^2)^2 + (z-L)^2}{4zL} \end{aligned}$$

where E is a total shock wave energy.

Shock wave collision in the bulk: entropy production

$$S \geq S_{\text{trapped}} \approx \pi \left(\frac{L^3}{G_5} \right)^{1/3} (2EL)^{2/3}$$

Shock wave collision in the bulk: entropy production

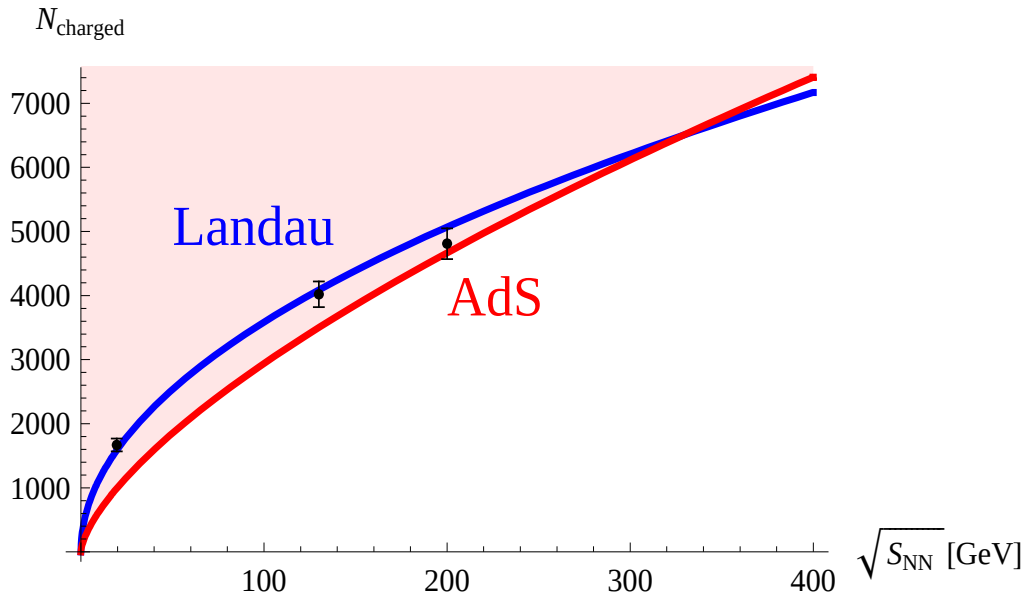

Jet propagation in nuclear matter

- Modifications of Altarelli-Parisi cascading due to decoherence and resulting pattern of energy loss.
- Cherenkov gluon single and double decays

- A.L., V. Nechitailo, Eur.Phys.J. C71 (2011) 1537; Nucl.Phys. A855 (2011) 380
- M. Alfimov, A.L., arXiv:1011.0340; arXiv:1106.5231

In-medium QCD cascade

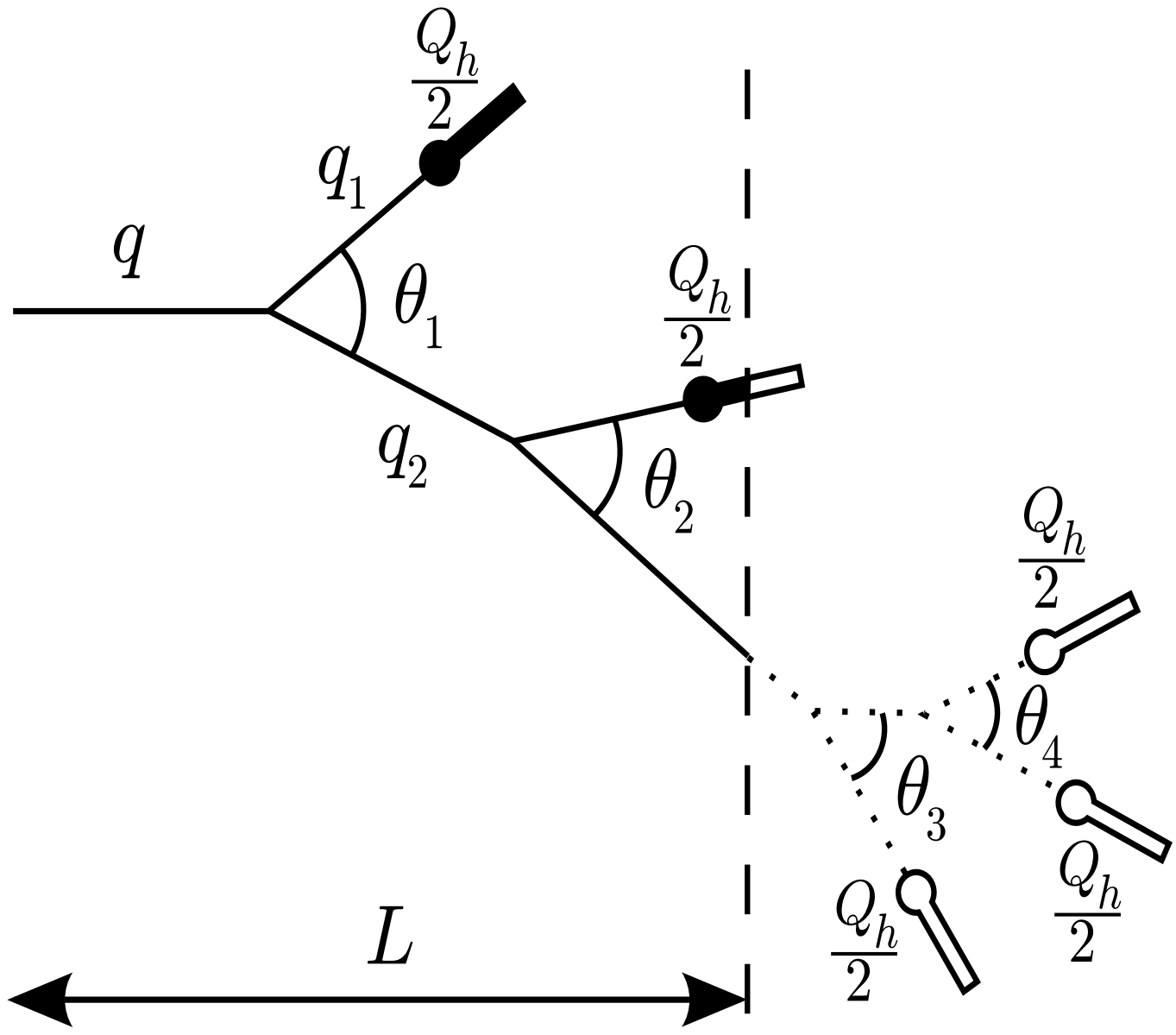

In-medium QCD cascade: models

- Two types of QCD cascades:
  - Cascade driven by degradation of virtuality (DGLAP)
  - Cascade driven by medium-induced particle production (similar to electromagnetic showers in matter)

- Rigorous description combining both effects is currently not available.
  Medium effects are taken into account by phenomenological "deformations"of one of the two basic alternatives

- Most studies "deform"the DGLAP evolution.

In-medium QCD cascade: models

- "Pionization"

  Dremin I.M. *JETP Lett.* **31** 185 (1980)
  Dremin I.M., A.L. *Sov. Journ. Nucl. Phys.* **35** 247 (1982)
  A.L., Ostrovsky D.M. *Phys. Atom. Nucl.* **60** 110 (1997);
  62 701 (1999)

- PYQUEN

  I.P. Lokhtin, A.M. Snigirev *Eur. Phys. J.* **C45** (2006), 211

- JEWEL

  Zapp K, Ingelman G, Rathsman J, Stachel J, Wiedemann U A,
  Eur. Phys. J **C60** 617 (2009)

- QPYTHIA

  Armesto N, Cunqueiro L, Salgado C A, *Eur. Phys. J* **C63** 679 (2009)

- QHERWIG

Main ingredients of the model

- Setup same as in JEWEL.
- Timelike mass-ordered QCD cascade with initial energy E_0 and virtuality Q_0^2 stopping at final virtuality $Q_h^2/4$.
- Angular ordering switched off for vertices generated inside the medium.
- Effect of nonradiative energy losses taken into account both for intercascade and final gluons.
- Medium-induced radiative losses not taken into account.

Mass-ordered QCD cascade

- Sequence of decays $q \to q_1 + q_2$
- Lifetime of the parton $\tau = E\left(\frac{1}{Q^2} - \frac{1}{Q^2_{\rm par}}\right)$
- Exact restrictions on $z = E_1/E$ from kinematics

$$\tilde{z}_-(E, Q^2|\ Q_1^2, Q_2^2) < z < \tilde{z}_+(E, Q^2|\ Q_1^2, Q_2^2)$$

$$\tilde{z}_\pm(E, Q^2|\ Q_1^2, Q_2^2)) = \frac{1}{2}\left(1 + \frac{q_+ q_-}{Q^2} \pm \sqrt{\left(1 - \frac{Q^2}{E^2}\right)\left(1 - \frac{q_+^2}{Q^2}\right)\left(1 - \frac{q_-^2}{Q^2}\right)}\right)$$

$q_\pm = \sqrt{Q_1^2} \pm \sqrt{Q_2^2}$.

- Angular ordering $\theta_4 < \theta_3$ but $\theta_2 \not< \theta_1$

Mass-ordered QCD cascade

- Simplified restrictions on $z = E_1/E$ from kinematics used in computing the Sudakov formfactor

$$z_-(E, Q^2|\ Q_h^2) < z < z_+(E, Q^2|\ Q_h^2)$$

$$z_\pm(E, Q^2|\ Q_h^2) \equiv \tilde{z}_\pm\left(E, Q^2|\ \frac{Q_h^2}{4}, \frac{Q_h^2}{4}\right) = \frac{1}{2}\left(1 \pm \sqrt{\left(1 - \frac{Q^2}{E^2}\right)\left(1 - \frac{Q_h^2}{Q^2}\right)}\right)$$

- The main quantity determining the structure of the cascade is the Sudakov formfactor

$$S\left(Q^2, E|Q^2_{\rm par}; Q_h^2\right) = \exp\left[-\int_{Q^2}^{Q^2_{\rm par}} \frac{dt^2}{t^2} \int_{z_-(E,\ t^2|\ Q_h^2)}^{z_+(E,\ t^2|\ Q_h^2)} dz \right.$$

$$\left. \times\ \frac{\alpha_s[z(1-z)t^2]}{2\pi} N_c \left(\frac{1}{z(1-z)} - 2 + z(1-z)\right)\right]$$

- $S\left(Q^2, E|Q^2_{\rm par}; Q_h^2\right)$ is the probability of having no decays in between the parent scale $Q^2_{\rm par}$ and a candidate scale Q^2 .

Numerical procedure

- One draws the scale Q^2 at which the gluon under consideration branches into two new gluons. Let us note that at this step one fixes the lifetime of the gluon $\tau = E(1/Q^2 - 1/Q^2_{\rm par})$.
- One draws the value of the splitting variable z determining the energies of the offspring gluons $E_1 = zE$ and $z_2 = (1-z)E$.
- With the energies of the offspring gluons fixed, one draws their final invariant masses $Q^2_{1,2}$ and, therefore, fix their lifetimes

$$\tau_{1,2} = E_{(1,2)}\left(1/Q^2_{(1,2)} - 1/Q^2\right)$$

- The values of $Q^2_{1,2}$ are accepted if they do not violate the condition

$$\tilde{z}_-(E, Q^2|\ Q^2_1, Q^2_2) < z < \tilde{z}_+(E, Q^2|\ Q^2_1, Q^2_2)$$

- If necessary, one ensures angular ordering by drawing the splitting variables for the decays of the offspring gluons $z_{1,2}$ and accepting them if

$$z_{1,2}(1 - z_{1,2}) > \frac{1-z}{z}\left(\frac{Q^2_{1,2}}{Q^2}\right)$$

Decoherence

- Angular ordering follows from quantum coherence based on covariant
  conservation of color

- In the hot zone the cascade develops in random color field, so that
  the color is no longer conserved and coherence and, consequently,
  angular ordering is expected to be broken

- In QGP the time scale for color rotation t_c is much faster than that of
  the momentum change t_p

$$\begin{aligned} t_p &\approx \left[4\alpha_s^2 T \ln(1/\alpha_s)\right]^{-1} \\ t_c &\approx \left[3\alpha_s T \ln(m_E/m_M)\right]^{-1}, \end{aligned}$$

A.V. Selikhov, M. Gyulassy, *Phys. Rev.* **C49** (1994), 1726

Changes in the branching pattern

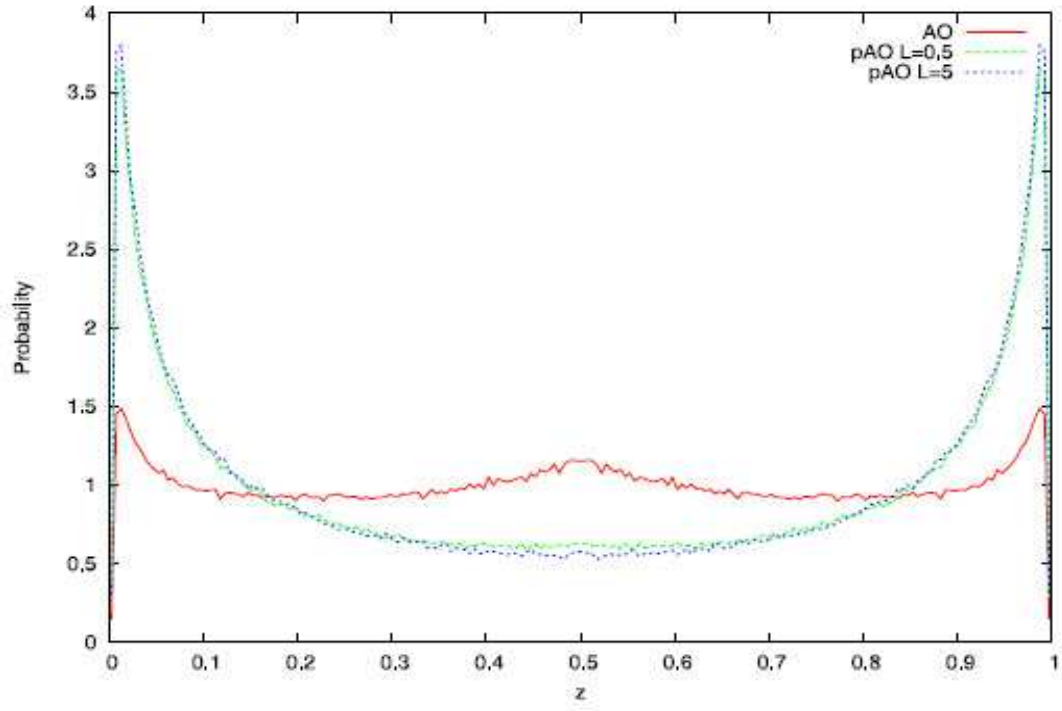

Distribution in the energy splitting variable z

- Global angular ordering, red, solid
- Partial angular ordering, green, dashed
- $L = 5$ fm, partial angular ordering, blue, dotted.

$\Rightarrow$ Enhanced production of soft particles

Rapidity distribution $P(y)$ of final prehadrons

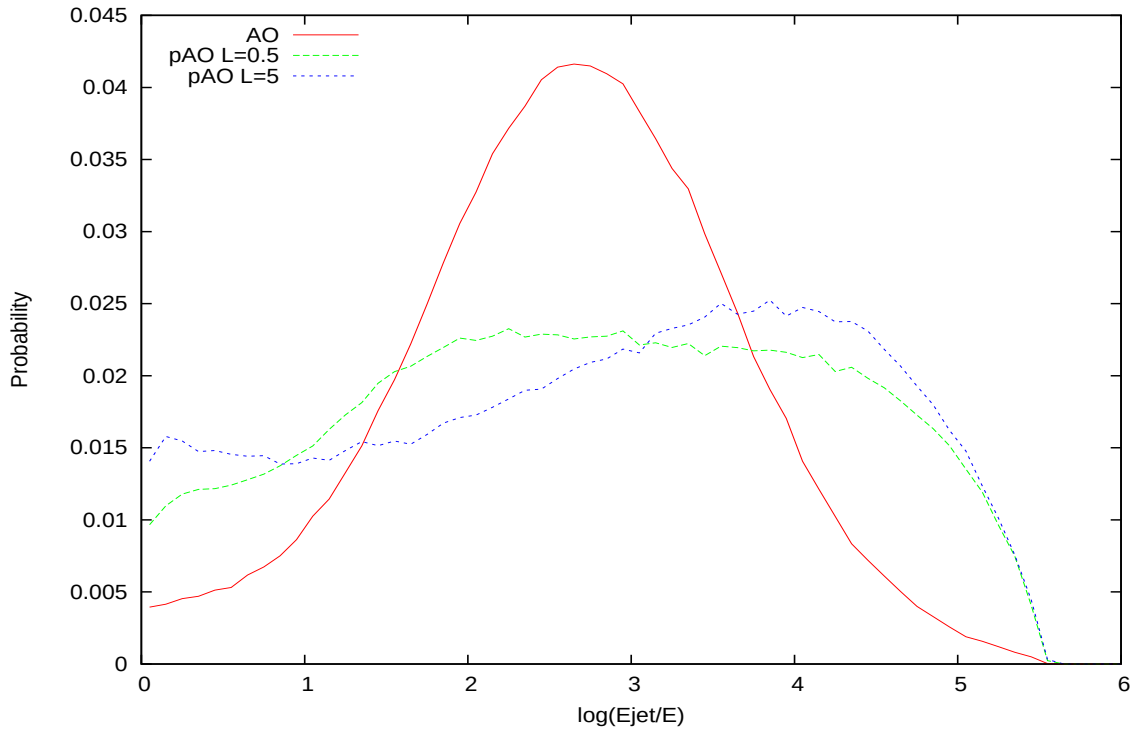

- $L = 0$ fm, full angular ordering, red, solid
- $L = 0.5$ fm, partial angular ordering, green, dashed
- $L = 5$ fm, partial angular ordering, blue, dotted.

$\Rightarrow$ Substantial softening of rapidity distribution already at times $\lesssim 1$ fm

- Soft particles form first (inside-outside cascade)

- Decoherence due to random impact from the medium disrupts angular ordering

- One gets more soft particles at larger angles within the hot zone

COLLISIONAL LOSSES

- Probability distribution for collisional energy losses ΔE_c of intercascade gluons per unit length (1 fm):

$$\mathcal{P}(\Delta E_c|\,\mu_c,\sigma_c) = \frac{1}{2}\left[1-\mathrm{erf}\left(\frac{\mu_c}{\sigma_c\sqrt{2}}\right)\right]\delta(\Delta E_c) + \frac{1}{\sqrt{2\pi\sigma_c^2}}\exp\left\{-\frac{(\Delta E_c-\mu_c)^2}{2\sigma_c^2}\right\}\Theta(\Delta E_c)$$

  In our computations we used $\mu_c = \sigma_c = 1\ \mathrm{GeV}$.

- Energy losses of final prehadrons $\Delta E_c = 1$ GeV/fm .

- Particle considered stopped if its energy reaches a critical value of $E_{\mathrm{crit}} = Q_h/2$.

Relative yield of prehadrons formed inside the medium

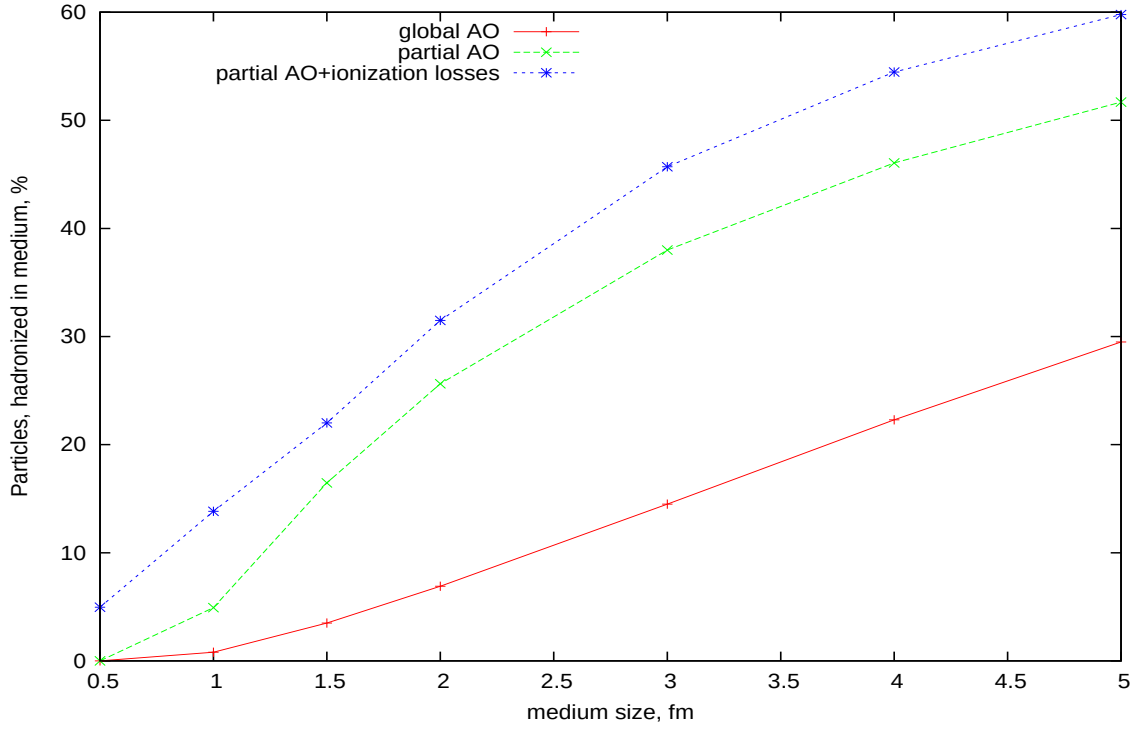

- Global angular ordering, red, solid
- Partial angular ordering, green, dashed
- Partial angular ordering and collisional losses, blue, dotted.

$\Rightarrow$ Prehadron formation inside the fireball enhanced

- All existing models assume hadronization taking place in the vacuum

$\Downarrow$

- We see, that a significant yield of prehadrons is formed inside the hot zone

$\Downarrow$

- Clear necessity to modify description of hadronization of QCD jets in the medium

Relative yield of particles stopped inside the medium

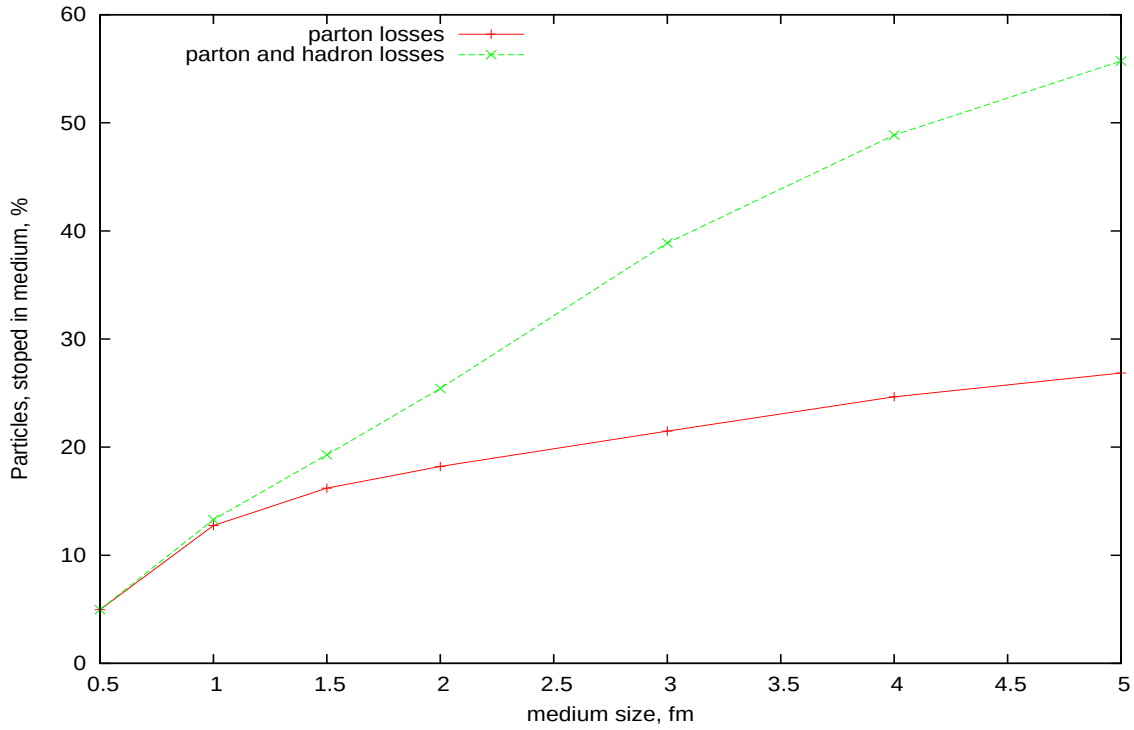

- Parton losses, red, solid
- Parton and hadron losses, green, dashed

$\Rightarrow$ The effect is especially important for final prehadrons formed inside the fireball

Mean jet multiplicity as a function of medium size

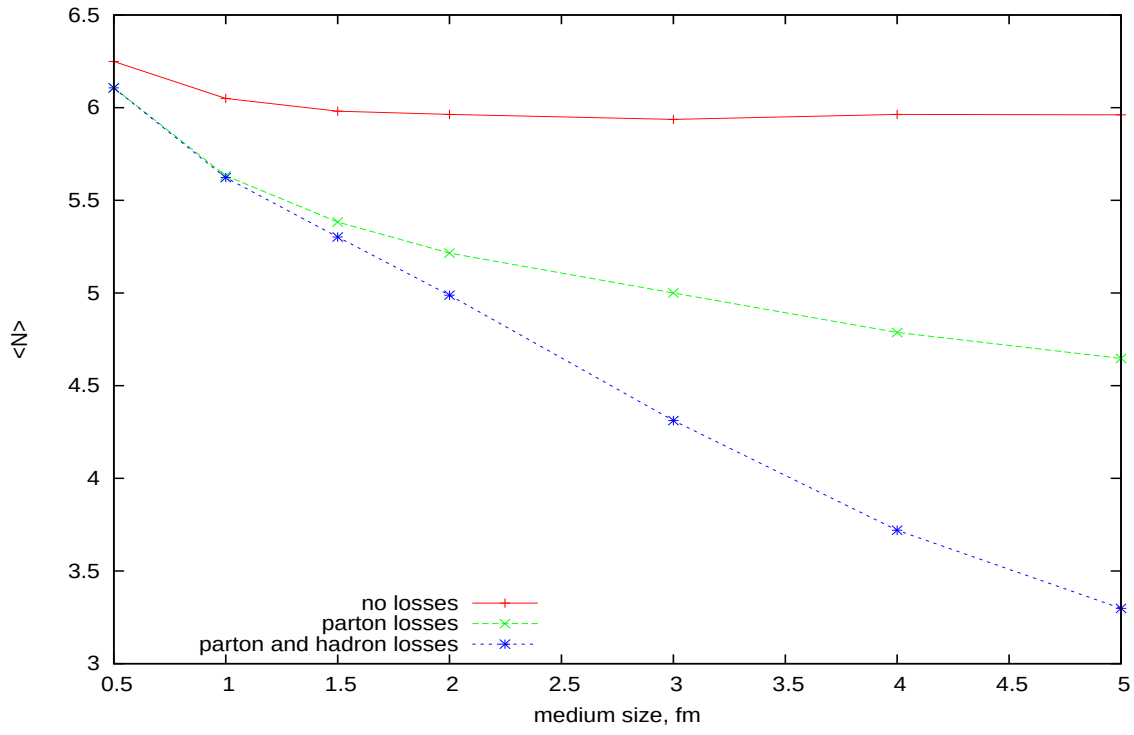

- No losses, red, solid
- Intracascade parton losses, green, dashed
- Intracascade and final state losses, blue, dotted.

Mean jet energy as a function of medium size

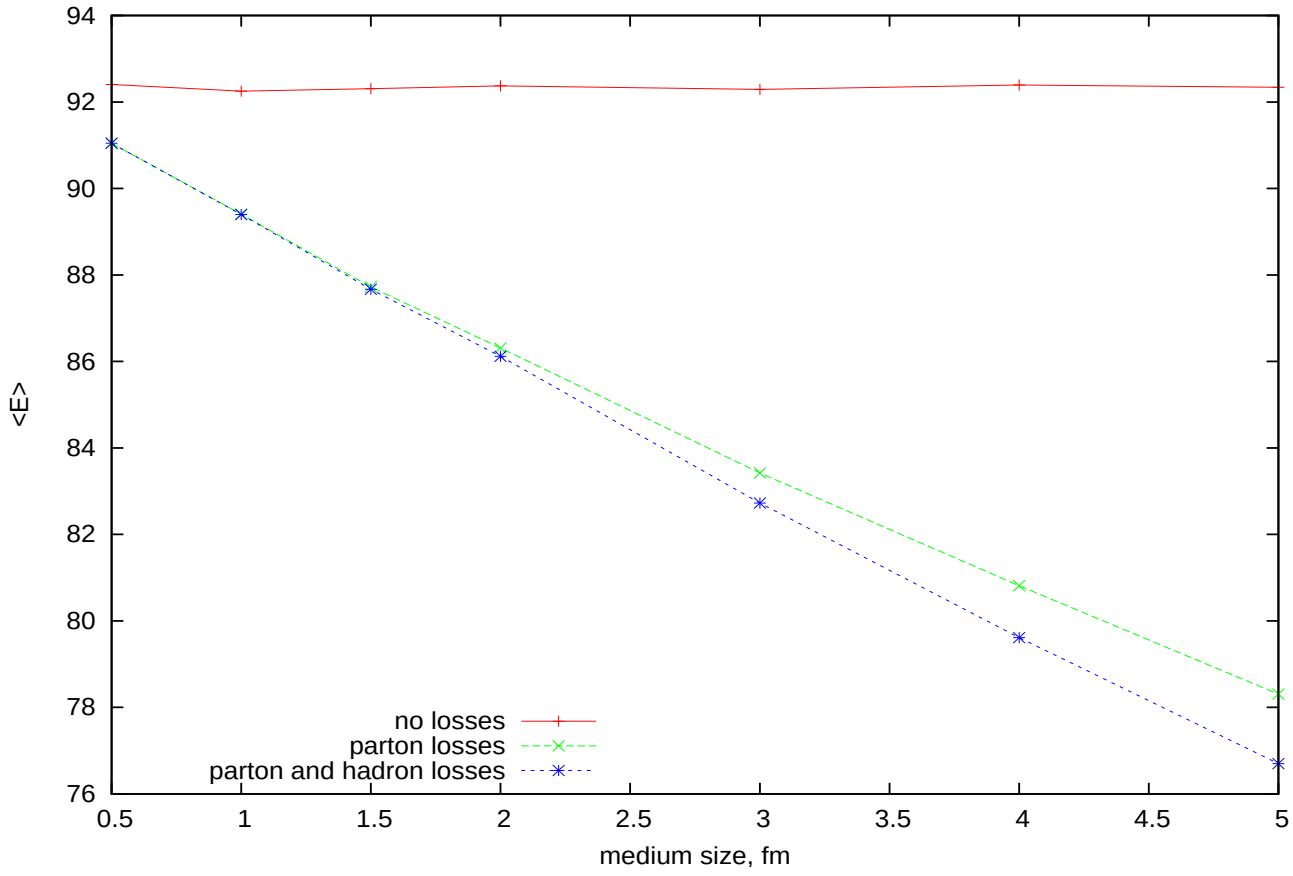

- No losses, red, solid
- Intracascade parton losses, green, dashed
- Intracascade and final state losses, blue, dotted.

Rapidity distribution $P(y)$ of final prehadrons with collisional losses

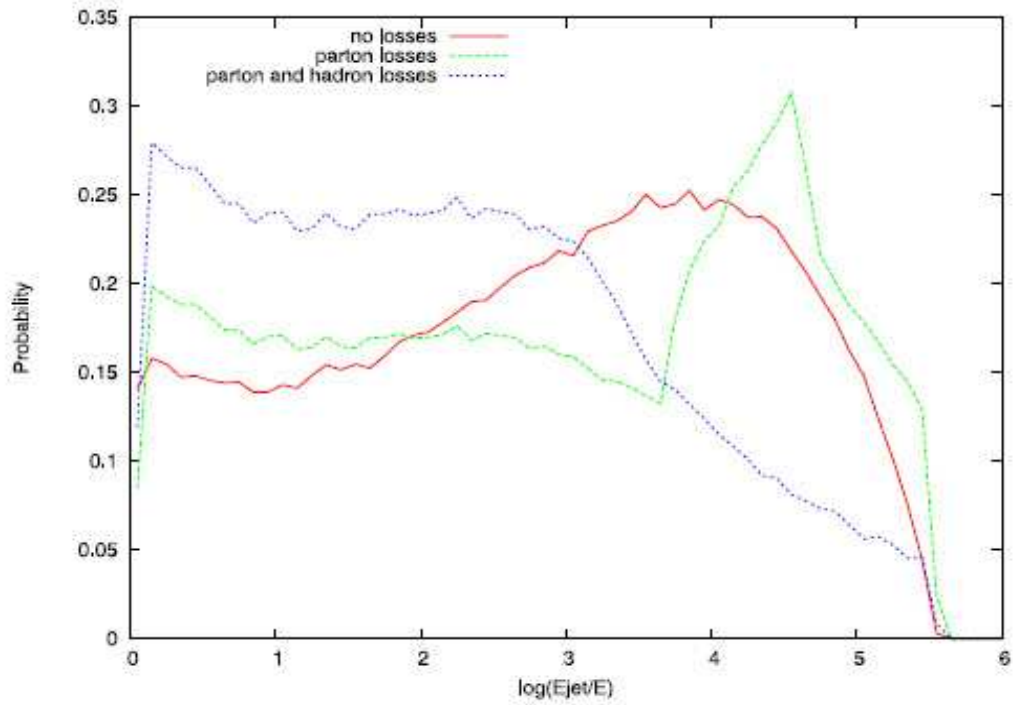

- $L = 0$ fm, full angular ordering, red, solid
- $L = 0.5$ fm, partial angular ordering, green, dashed
- $L = 5$ fm, partial angular ordering, blue, dotted.

$\Rightarrow$ Substantial hardening of rapidity distribution due to collisional losses

EXPERIMENTAL RESULTS ON JET STRUCTURE AT LHC

B. Wyslouch, talk at QM2011

$$p_T^{\parallel} = \sum_{\text{Tracks}} -p_T^{\text{Track}} \cos\left(\phi_{\text{Track}} - \phi_{\text{Leading Jet}}\right)$$

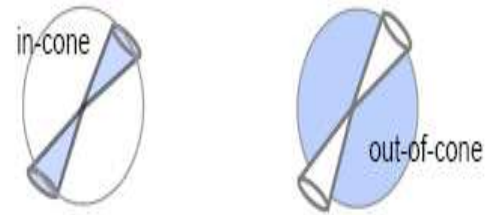

0-30% Central PbPb

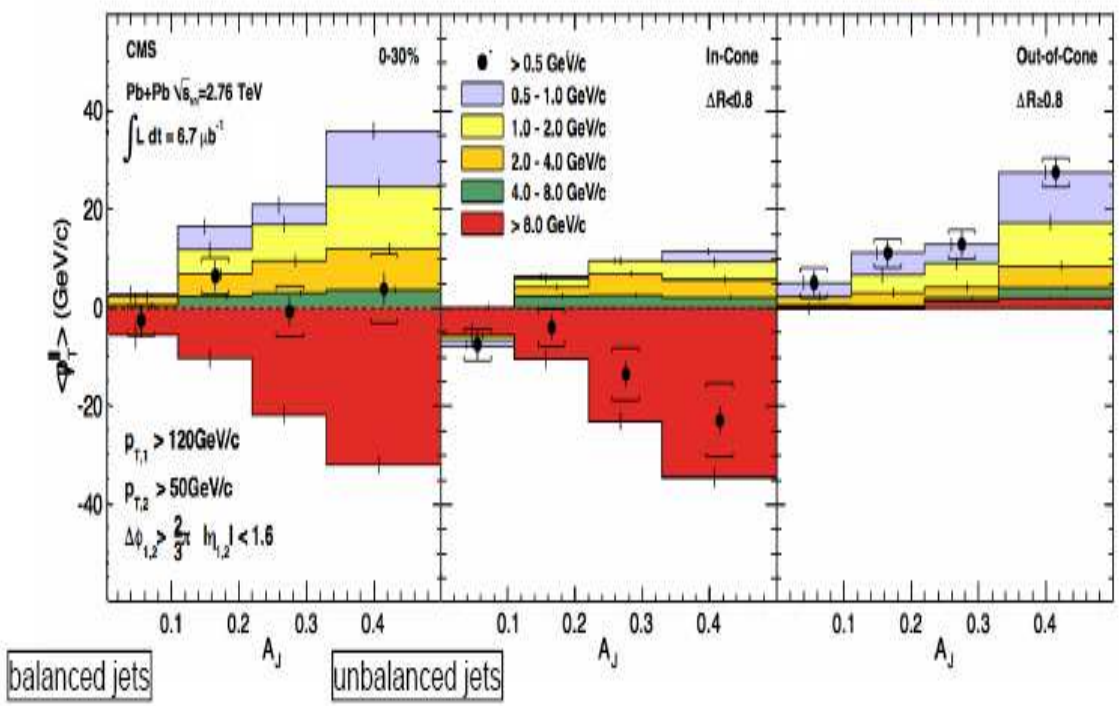

Low p_T, full acceptance
Momentum is balanced

In-cone large momentum imbalance at high p_T
Consistent with calorimetry

Out-off-cone low p_T particles balance the complete event

Fragmentation functions

- Updated jet algorithm: Particle Flow, Anti-k_T, R=0.3
- Charged tracks, p_T^{Track} >4 GeV/c, jets with p_T^{Jet} =40-300 GeV/c

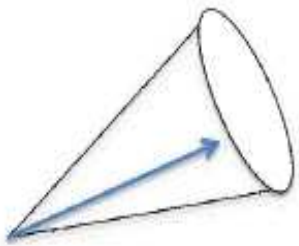

$$\xi = \ln\left(\frac{p_T^{Jet}}{p_T^{Track}}\right)$$

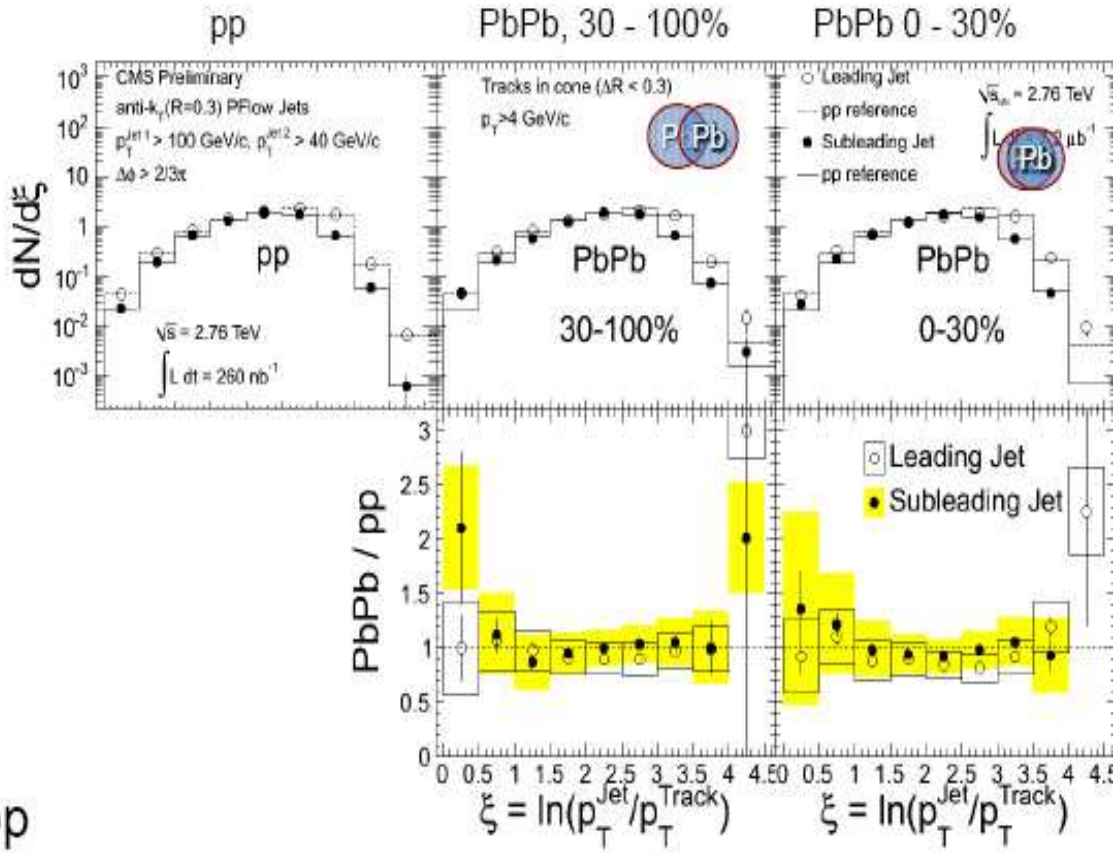

- Compare PbPb to pp
  - Fragmentation function similar between PbPb and pp
  - Jets fragment in the vacuum

Y. Yilmaz (Fri), C. Roland (Wed), M. Nguyen (Fri)

Conclusions

- Effects of medium-induced disruption of angular ordering of the mass-ordered gluon cascade and non-radiative energy loss inside the hot fireball studied within the Monte Carlo model
- Crucial role of the inside-outside nature of the cascade
- Results in qualitative agreement with LHC data

Cherenkov radiation of gluons

- Interaction of usual gluons with Cherenkov ones is considered
- Cherenkov gluons are those with $|\mathbf{q}| = \sqrt{\varepsilon}\omega$, where $\varepsilon > 1$
- Simple model for permittivity:

$$\begin{aligned} \varepsilon^{ab}(\omega, \mathbf{k}) &\rightarrow \delta^{ab}\varepsilon(\omega) \\ \varepsilon(\omega) &= \varepsilon > 1,\ \omega < \omega_0 \\ \varepsilon(\omega) &= 1,\ \omega > \omega_0 \end{aligned}$$

Values of parameters: $\varepsilon = \simeq 5$ and $\omega_0 = 3\ \mathrm{GeV}$
(I.M. Dremin et al., *Nucl.Phys* **A826** (2009), 190)

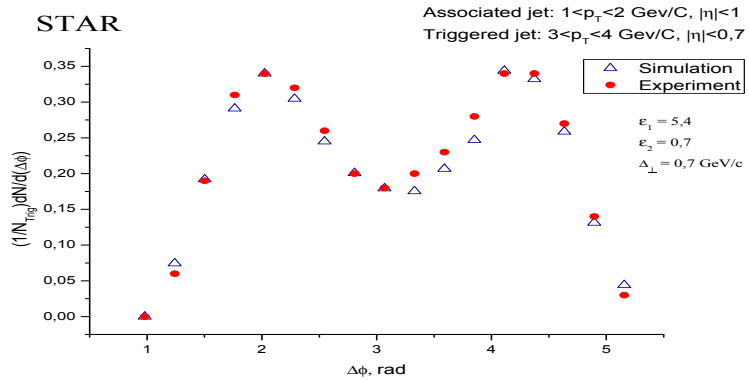

Cherenkov radiation of quark currents

$$q(p) \to q(q-p) + \tilde{g}(q)$$

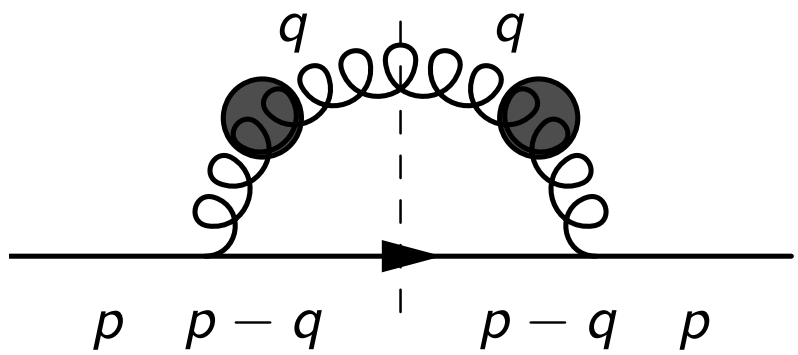

Cherenkov angle:

$$\cos\theta = \frac{1}{\sqrt{\varepsilon}}\left(1 + \frac{\varepsilon - 1}{2}\frac{\omega}{E}\right)$$

Transverse broadening:

$$|\mathbf{p}'_\perp| = \omega\sqrt{\frac{\varepsilon-1}{\varepsilon}}\left[1 - \frac{\omega}{E} - \frac{\varepsilon-1}{4}\left(\frac{\omega}{E}\right)^2\right]^{1/2}\Bigg|_{\omega/E\to 0} \sim \omega\sqrt{\frac{\varepsilon-1}{\varepsilon}}$$

Cherenkov radiation of quark currents

$$q(p) \to q(q-p) + \tilde{g}(q)$$

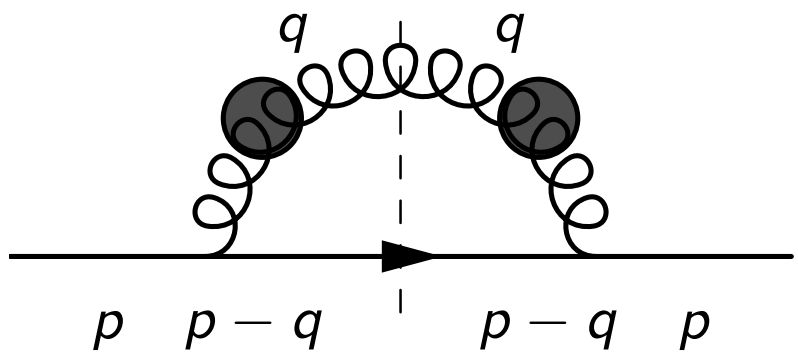

decay rate:

$$\gamma_{q\to q\tilde{g}}(\omega|E) = \alpha_s \frac{(N_c^2-1)}{2N_c}\left(1-\frac{1}{\varepsilon}\right)\left(1-\frac{\omega}{E}+\frac{\varepsilon+1}{4}\frac{\omega^2}{E^2}\right)$$

Cherenkov radiation of quark currents

$$q(p) \to q(q-p) + \tilde{g}(q)$$

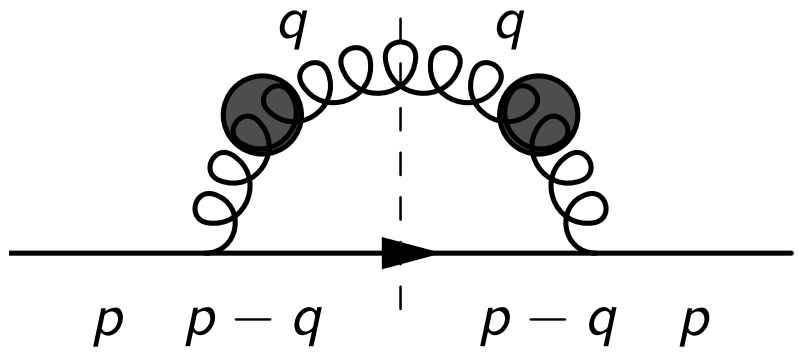

Energy spectrum:

$$P_{q\to q\tilde{g}}(\omega|E) = \omega\, \gamma_{q\to q\tilde{g}}(\omega|E)$$

Cherenkov radiation of quark currents

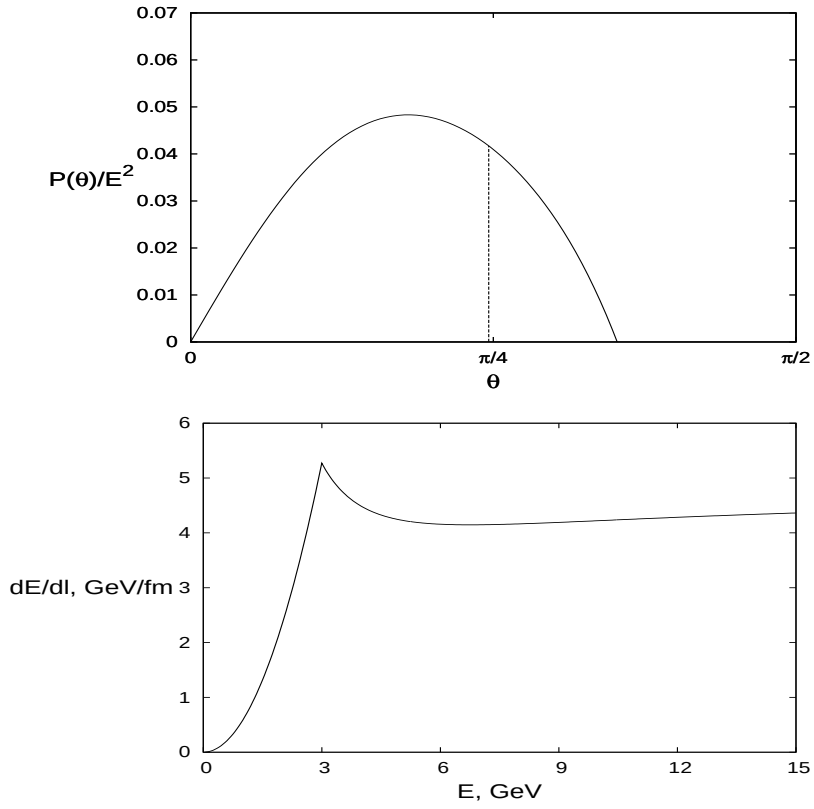

- $\Uparrow$: angular pattern of energy flow of the quark Cherenkov decay, $\varepsilon = 5$, $\omega_0 = 3\ \mathrm{GeV}$.
- $\Downarrow$: Cherenkov energy loss, $\varepsilon = 5$, $\omega_0 = 3\ \mathrm{GeV}$.

Cherenkov radiation of gluon currents

$$g(p) \to g(q-p) + \tilde{g}(q)$$

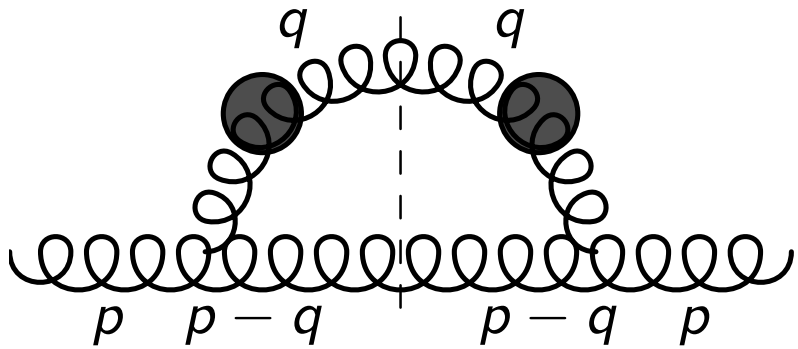

decay rate:

$$\begin{aligned}\gamma_{g\to g\tilde{g}}(\omega|E) &= \alpha_s N_c \left(1-\frac{1}{\varepsilon}\right)\left(1-\frac{\omega}{E}-\frac{\varepsilon-1}{4}\frac{\omega^2}{E^2}\right)\\ &\times \left[1+\frac{1}{2}\left(\varepsilon+\frac{\varepsilon+1}{1-\frac{\omega}{E}}+\frac{\varepsilon}{\left(1-\frac{\omega}{E}\right)^2}\right)\frac{\omega^2}{E^2}+\frac{(\varepsilon+1)^2}{8\left(1-\frac{\omega}{E}\right)^2}\frac{\omega^4}{E^4}\right.\end{aligned}$$

Cherenkov radiation of gluon currents

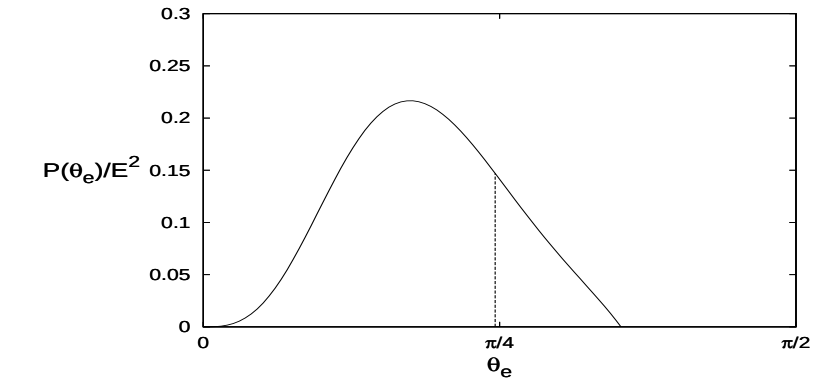

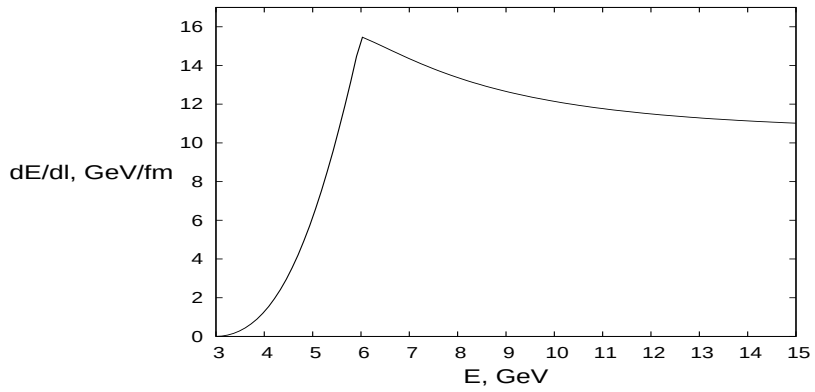

- $\Uparrow$: angular pattern of energy flow of the gluon Cherenkov decay, $\varepsilon = 5$, $\omega_0 = 3\ \mathrm{GeV}$.
- $\Downarrow$: Cherenkov energy loss, $\varepsilon = 5$, $\omega_0 = 3\ \mathrm{GeV}$.

Double Cherenkov decay of gluon currents

$$g(p) \to \tilde{g}(q-p) + \tilde{g}(q)$$

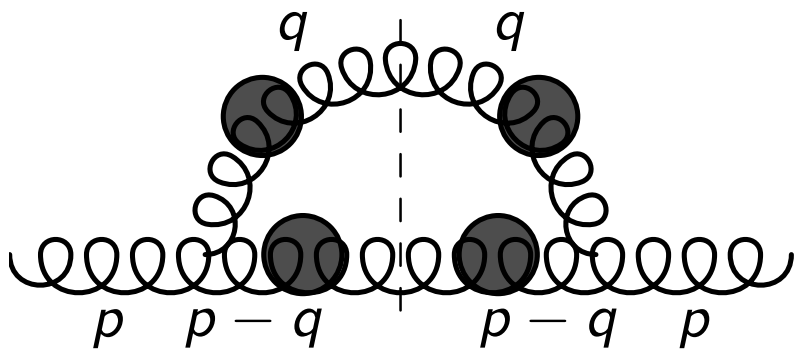

Cherenkov angle:

$$\cos\theta = \sqrt{\varepsilon} - \frac{\varepsilon - 1}{2\sqrt{\varepsilon}}\frac{E}{\omega}$$

Restriction of the energy of the Cherenkov gluon:

$$\frac{1}{2} - \frac{1}{2\sqrt{\varepsilon}} < \frac{\omega}{E} < \frac{1}{2} + \frac{1}{2\sqrt{\varepsilon}}$$

Double Cherenkov decay of gluon currents

$$g(p) \to \tilde{g}(q-p) + \tilde{g}(q)$$

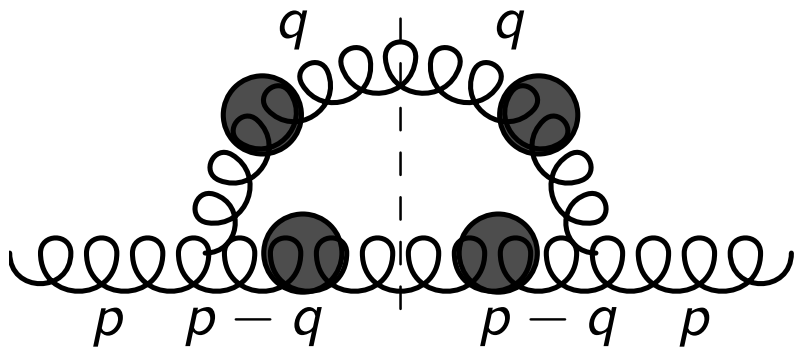

decay rate:

$$\gamma_{g\to\tilde{g}\tilde{g}}(\omega|E) = \frac{\alpha_s N_c}{2}\left[1-\left(\sqrt{\varepsilon}-\frac{\varepsilon-1}{2\sqrt{\varepsilon}}\frac{E}{\omega}\right)^2\right]$$

$$\times \left[1+\varepsilon\frac{\omega^2}{E^2}+\frac{\frac{\omega^2}{E^2}}{(1-\frac{\omega}{E})^2}+\varepsilon\left(1-\frac{\varepsilon-1}{2\varepsilon}\frac{1}{1-\frac{\omega}{E}}+\frac{\frac{\omega^2}{E^2}}{1-\frac{\omega}{E}}\right.\right.$$

Double Cherenkov decay of gluon currents

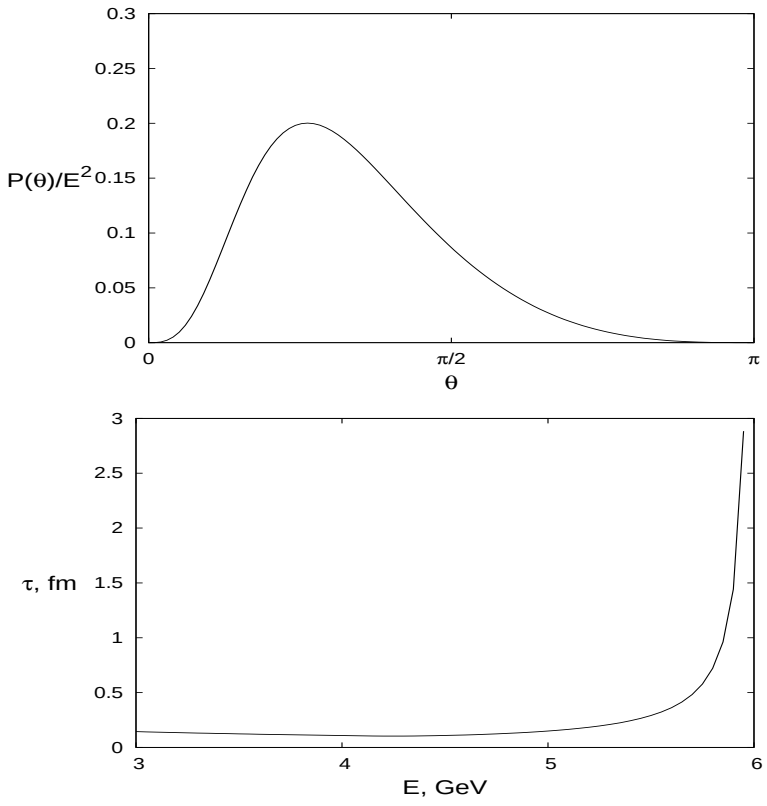

- $\Uparrow$: angular pattern of energy flow of the gluon Cherenkov decay, $\varepsilon = 5$, $\omega_0 = 3\ \mathrm{GeV}$.
- $\Downarrow$: Gluon lifetime, $\varepsilon = 5$, $\omega_0 = 3\ \mathrm{GeV}$.

Generic pattern of Cherenkov energy loss

- For quark currents the only available decay channel is the single Cherenkov decay. The corresponding energy loss is non-negligible but subleading with respect to that of the gluon current.
- For incident gluons with energy in the interval $0 < E < 2\omega_0$ the leading contribution to the energy loss comes from the double Cherenkov decay. The corresponding pattern of angular correlations corresponds to two peaks around the direction of propagation of the decaying gluon. There also exists a small contribution due to single Cherenkov decay.
- At the threshold energy $E = 2\omega_0$ there takes place a regime switch between the predominant double Cherenkov decay at $E < 2\omega_0$ to the single Cherenkov decay of quark and gluon currents at $E > 2\omega_0$ where one expects the possible appearance of the third hump corresponding to the incident particle. At the threshold $E = 2\omega_0$ the there takes place the following change in the Cherenkov angle:

Experimental data on two-particle azimuthal correlations

M.M. Aggarwal et al. (STAR) *Phys. Rev.* **C82** (2010), 024912

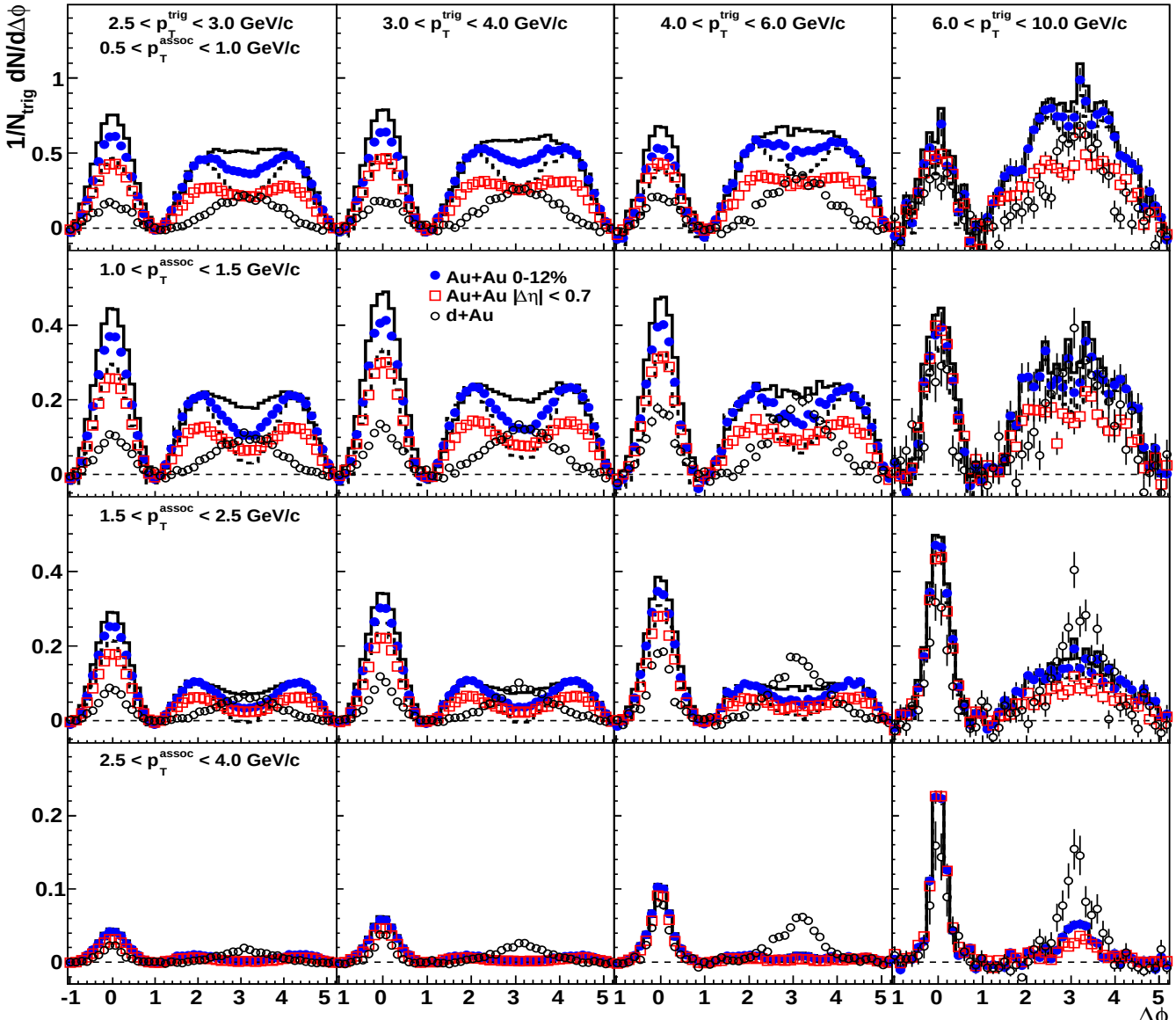

Color rainbow

Generalized linearized EOM for in-medium QCD

$$\begin{aligned} \triangle \mathbf{A}^a - \epsilon^{ab} \frac{\partial^2 \mathbf{A}^b}{\partial t^2} &= -\mathbf{j}^a, \\ \epsilon^{ab}(\triangle \Phi^b - \epsilon^{bc} \frac{\partial^2}{\partial t^2} \Phi^c) &= -\rho^a \end{aligned}$$

Diagonalization of ϵ^{ab}:

$$\epsilon \rightarrow \tilde{\epsilon} = U \epsilon U^{-1}$$

Eigenvalues:

$$\begin{aligned} \epsilon^{(1)} &\equiv \epsilon^* = \epsilon^{(\mathrm{d})} + 2\epsilon^{(\mathrm{o})}, \\ \epsilon^{(2),\cdots,(N_c^2-1)} &\equiv \epsilon^{**} = \epsilon^{(\mathrm{d})} - \epsilon^{(\mathrm{o})} \end{aligned}$$

Two Cherenkov angles:

$$\cos\theta^* = \frac{1}{v\sqrt{\epsilon^{(\mathrm{d})} + 2\epsilon^{(\mathrm{o})}}}, \quad \cos\theta^{**} = \frac{1}{v\sqrt{\epsilon^{(\mathrm{d})} - \epsilon^{(\mathrm{o})}}}$$

All this looked nice, but

- Experimental data very well described by azimuthal asymmetries

ALICE Collaboration arXiv:1105.3865

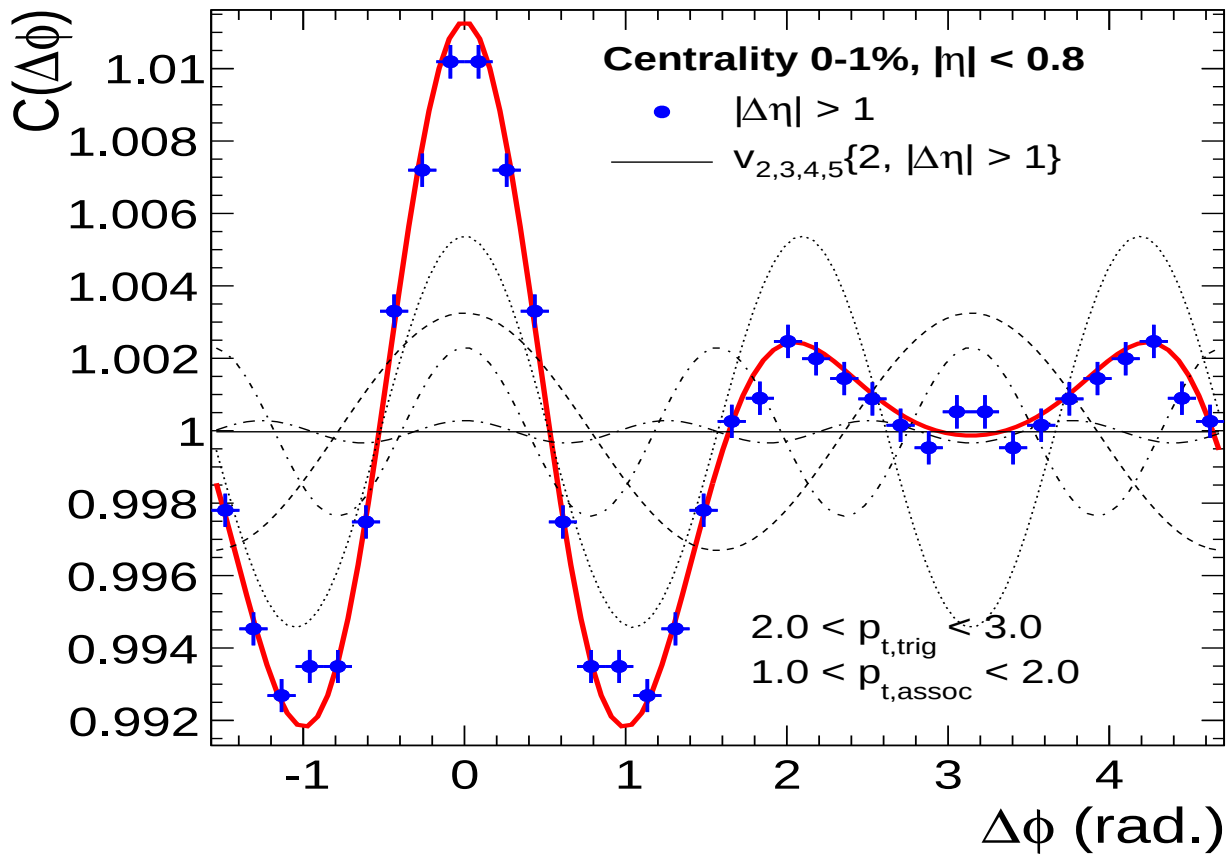

- No evidence for Cherenkov glue from lattice

F. Karsch et al., DESY 02-109

P.Petresczku, Nucl. Phys. (Proc. Suppl.) 106 (2002), 513

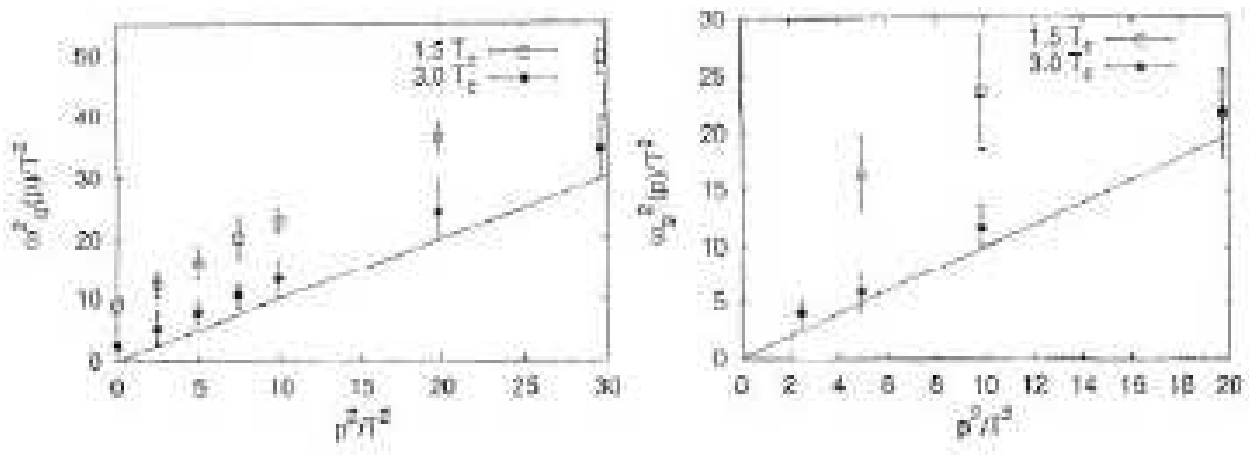

Fig. 5. The dispersion relation of quarks (left) and gluons (right) for temperatures $T = 1.5T_c$ and $3T_c$.